Copyright Warning & Restrictions

The copyright law of the United States (Title 17, United States Code) governs the making of photocopies or other reproductions of copyrighted material.

Under certain conditions specified in the law, libraries and archives are authorized to furnish a photocopy or other reproduction. One of these specified conditions is that the photocopy or reproduction is not to be "used for any purpose other than private study, scholarship, or research." If a, user makes a request for, or later uses, a photocopy or reproduction for purposes in excess of "fair use" that user may be liable for copyright infringement,

This institution reserves the right to refuse to accept a copying order if, in its judgment, fulfillment of the order would involve violation of copyright law.

Please Note: The author retains the copyright while the New Jersey Institute of Technology reserves the right to distribute this thesis or dissertation

Printing note: If you do not wish to print this page, then select "Pages from: first page # to: last page #" on the print dialog screen

ABSTRACT

Design, Fabrication and Characterization of Infrared Filters

by
Samiul Amin

In-situ temperature monitoring, mapping, and control have become significant in semiconductor processes. Temperature of these processes can be measured by making use of the thermal emission from substrates in the infrared region. Various methods have been proposed to provide multicolor infrared detection. One such method involves placing segmented infrared filters close to the focal plane. The present study aims at gaining an insight into the design, fabrication and characterization of infrared filters. Filters were designed and fabricated with peak transmission at 1.5, 3.0, and 4.5 μm. Extensive spectroscopic studies, using FTIR spectroscopy, have been performed in the infrared region, on the materials chosen for the filters - Si, SiO_2, and Al_2O_3. The spectral transmittance characteristics of the filters have also been studied using optical spectrometry to monitor their performance at the desired wavelengths.

DESIGN, FABRICATION AND CHARACTERIZATION OF INFRARED FILTERS

by
Samiul Amin

A Thesis
Submitted to the Faculty of
New Jersey Institute of Technology
in Partial Fulfillment of the Requirements for the Degree of
Master of Science in Electrical Engineering

Department of Electrical and Computer Engineering

October 1993

APPROVAL PAGE

Design, Fabrication and Characterization of Infrared Filters

Samiul Amin

Dr. N. M. Ravindra, Thesis Advisor — date
Associate Professor of Physics Department, NJIT

Dr. Walter F. Kosonocky, Thesis Advisor — date
Distinguished Professor
Foundation Chair of Optoelectronics and Solid State Circuits
Electrical and Computer Engineering, NJIT

Dr. Kenneth Sohn, Committee Member — date
Professor and Acting Associate Chairperson
Electrical and Computer Engineering, NJIT

BIOGRAPHICAL SKETCH

Author: Samiul Amin

Degree: Master of Science in Electrical Engineering

Date: August, 1993

Undergraduate and Graduate Education:

- Master of Science in Electrical Engineering
  New Jersey Institute of Technology, Newark, NJ, 1993

- Bachelor of Science in Electrical Engineering
  Bangladesh University of Engineering and Technology
  Dhaka, Bangladesh, 1989

Major: Electrical Engineering

This thesis is dedicated to
my Parents and Dr. N. M. Ravindra

ACKNOWLEDGEMENT

The author wishes to express his deep reverence and appreciation to his thesis advisor, Dr. N.M. Ravindra for his patience, guidance, and advice throughout the project.

The author would also like to express his sincere gratitude to his supervisor, Dr. Walter F. Kosonocky, for his guidance and moral support throughout the course of this research. In addition, special thanks to Dr. K. Sohn, for serving as member of the committee.

The financial support of Advanced Research Projects Agency (ARPA) under Contract No. F33615-92-C-5817 through Wright Patterson Airforce Base is acknowledged with thanks.

The author appreciates the efforts of the Dr. Bawa Singh, Ramazan Soydan, and Peter Zanzucci of the Thin Films Division at David Sarnoff Research Center(DSRC). The author is also thankful to Dorothy Hoffman, an independent consultant to the project for sharing her knowledge, experience, and expertise during the design and fabrication of the filters. Special thanks to Gil Green of DSRC for his help in making the different adaptors for the optical monitor system. The author extends his gratitude to Advanced Fuel Research Inc. for performing FTIR spectroscopic studies on SiO_2 samples.

The author would also like to thank members of 414T for providing a pleasant working environment. Special thanks to Professor F. M. Tong, Srinivasa Munukutla, Vipul Patel, Louis Casas, Mukund Gundanna, Sajid Haque, Showkat Haque, and Anitha Kodali for their good spirits.

The author is deeply indebted to his parents, uncles and aunts for their constant encouragement and moral support.

TABLE OF CONTENTS

LIST OF FIGURES

Figure Page

LIST OF TABLES

CHAPTER 1
INTRODUCTION

1.1 An Overview

Among the many new techniques which have become significant in applications beyond the laboratory is the field known as infrared[1]. The term infrared, as generally known, is applied to devices which depend, for their basic information, on the electromagnetic energy of wavelength between 0.7 to 1,000 μm which is reflected from, absorbed by, or emitted by objects of interest. With the development of better photoconductive detectors, it has been increasingly important to match the spectral bandpass of a system with the detection range. The principal means of accomplishing this is to use optical filters[2]. Here, a study has been carried out on the design, fabrication, and characterization of narrow band-pass infrared filters.

The filters were fabricated as part of the project "Multi-wavelength imaging and pyrometry (MWIP) for semiconductor process monitoring and control", that has been funded by ARPA. The design of the filters were performed by Dorothy Hoffman. The optical characterization of the materials selected for the filter was performed by Pete Zanzucchi at David Sarnoff Research Center (DSRC) and Jim Markham at Advanced Fuel Research (AFR). The filters were fabricated in the Thin Films Division of the David Sarnoff Research Center under the supervision of Bawa Singh and Ram Soydan.

The infrared filters are part of a system intended for use in in-situ monitoring of the radiant flux emitted by a semiconductor wafer during process. The system is designed for remote measurements of wafer temperatures in the range of 50 to 1000°C. The system will be configured to

operate with upto six narrow band-pass filters. The center wavelengths and the bandwidths of these filters have been selected for optimum response over the temperature range of interest. To achieve narrow bandwidth and peak transmission at the desired wavelength, Si, SiO_2 or Al_2O_3, and Al were considered as the materials of choice. The design for the filters have been made considering these materials. Deposition conditions for each material have been obtained and optimized for greater process repeatability. Spectroscopic studies have been performed on the films to obtain refractive index and extinction co-efficient data. This information has been used to obtain a new set of design parameters for the filters. The layers were deposited by electron-beam assisted thermal evaporation in vacuum.

An important parameter for filter fabrication is the control of the deposition of layers so that they have the characteristics required by the filter design[3]. Optical monitoring is the most accurate and widely used technique for the measurement and control of optical thin films during deposition[4]. This is due to the fact that the method measures the optical thickness of the film rather than its mass. Thus any variations in the film structure that may cause the refractive index of the film to vary are taken into account.

1.1.2 Specification of the Filters

The specifications for the filters that have been fabricated are:

Center Wavelength	1.5 to 4.5μm
Bandwidth	5 to 500μm
Peak Transmittance	40-60%
Rejection Ratio	<0.1%
Substrate	Intrinsic Si, polished on both sides

To obtain these specifications, great care must be taken to set up deposition conditions so that the layers are of uniform density throughout the whole filter. Thickness monitoring of the depositing layers is very important for filter fabrication.

1.1.3 IR Filter Applications

Infrared filters are usually part of an optical system - they are rarely used by themselves. Compared with a grating monochromator, the thin-film filter with the same bandwidth is capable of collecting two to three orders higher the amount of energy collected by the monochromator, provided the rest of the system is correctly designed around it[5]. Another advantage of the IR filter is that it can be of smaller size than the monochromator and still have a very significant increase in energy transfer over it. Infrared filters, as part of optical systems, have found a wide range of applications, both in military and industrial sectors[6][7].

(a) Radiometry: Infrared detectors are extensively used as remote temperature indicators. In military, these sensors rely on spectral signatures for target identification and tracking. In general, such signatures include the spectral, spatial, and temporal characteristics of the target radiation. In industry, sensors are used for process control, noncontact dimensional determination, measurement of temperature of cutting tools, welding, and soldering operations.

(b) Spectroradiometry: This category has a wide range of applications in systems used for terrain analysis, poison gas detection, fuel vapor detection, analysis of gases and organic chemicals, control of oxygen content in Ge and Si, discovery of leaks in pipelines, determination of alcohol in breath and detection of oil in water. The immediate result of this spread of IR

spectrometry was the drawing up of spectra atlases of all pure substances and the application of them to the analysis of mixtures, the determination of structures, the study of molecular associations, and chemical reactions.

(c) Thermal imaging: This category has undergone a rapid growth because of the successful application of thermal imaging devices to nondestructive testing and inspection. This is widely applicable to military systems for reconnaissance and surveillance, submarine detection, detection of underground missile silos, and damage assessment.

(d) Search, track, and range: Infrared search and track systems are of vital importance in intrusion detection, bomber defense, missile guidance, and navigation and flight control. These systems operate equally well during the day or at night. Infrared techniques are very attractive for the early detection of forest fires.

(e) Medical applications: The skin is relatively transparent in the near infrared. As such, photographs made on infrared film, or observations with image convertor devices, yield valuable inormation about skin disorders, healing of wounds, and the condition of the superficial venous system. In addition to their use for the early detection of cancer, radiometers are being used as noncontact biosensors for astronauts, for studies of the physiological mechanisms of temperature sensation, and to detect the healing of wounds.

(f) Planetary studies: Information of two kinds may be obtained from a study of planets in the infrared region of the spectrum. First, the spectrum of light reflected or emitted by the planet may be analysed and the composition of the planet's atmosphere deduced from the presence of absorption bands of the gases involved[8]. Second, the effective temperature of the radiating surface of the planet may be deduced from radiometric measurements of the amount of energy it emits.

(g) Atmospheric studies: One of the more recent applications of infrared equipment is for the early detection of clear-air turbulence, that is, conditions in which an aircraft encounters severe turbulence despite the fact that visual and radar observations show no evidence of any convective cloud activity in the area. Infrared systems are also used for detection of environmental pollution, remote sensing of weather conditions, and measurement of the earth's heat balance.

1.2 Objectives of the current work

This study focuses on the design, fabrication, and characterization of narrow bandpass infrared filters. The thesis gives an overview of filter design and a spectroscopic study of the materials chosen for the filters. It describes the optical monitoring process for thickness control of the depositing layers. The thesis includes the experimental procedures used to fabricate and characterize the filters.

1.3 Organization of the Thesis

This thesis consists of studies on the design, fabrication, and characterization of infrared filters. Chapter 2 throws light on filter design and its dependence on layer thicknesses of each material. In Chapter 3, the fabrication process of the filters has been discussed with an emphasis on thickness monitoring. Chapter 4 concerns with the spectroscopic study of the materials chosen for the filters. Conclusions inferred from experimental data are presented in Chapter 5. Future work and recommendations are described in Chapter 6.

The various process programs used for filter fabrication and characterization are given in the Appendix.

CHAPTER 2
FILTER DESIGN

2.1 Introduction

A filter which possesses a region of transmission bounded on either side by regions of rejection is known as a band-pass filter. Depending on the width of the transmission region, one may distinguish between narrow-band and broad-band filters[9]. A typical narrow-band filter is the metal dielectric Fabry-Perot filter based on the Fabry-Perot interferometer. The thin-film Fabry-Perot filter has a pass-band shape which is triangular. It has been found possible to improve this shape by coupling simple filters in series. These coupled arrangements are known as multiple cavity filters or multiple half-wave filters. If two simple Fabry-Perot filters are combined, the resultant becomes a double cavity or double half-wave filter, abbrevaited as DHW filter. The design of the double cavity filter is described in this chapter.

2.2 Basic Theory

There are several conditions that have to be taken into account before designing a filter[5]. They are as follows:

(1) The amplitude reflectance of light at any boundary between two media is given by

$$(1-\rho)/(1+\rho) \qquad (2.1)$$

where ρ is the ratio of the refractive indices at the boundary.

(2) There is a phase shift of 180° when the reflectance takes place in a medium of lower refractive index than the adjoining medium and zero if the medium has a higher index than the one adjoining it.

(3) If the light is split into two components by reflection at the top and bottom surfaces of a thin film, then the beams will recombine in such a way that the resultant amplitude will be the difference of the amplitudes of the two components if the relative phase shift is 180°, or the sum of the amplitudes if the relative phase shift is either zero or a multiple of 360°. In the former case, the beams interfere destructively and in the latter constructively.

A basic type of thin-film structure is a stack of alternate high- and low-index films, all one quarter wavelength thick (Fig.2.1). Light which is reflected within the high-index layers will not suffer any phase shift on reflection, while those beams reflected within the low-index layers will suffer a change of 180°. The various components of the incident light

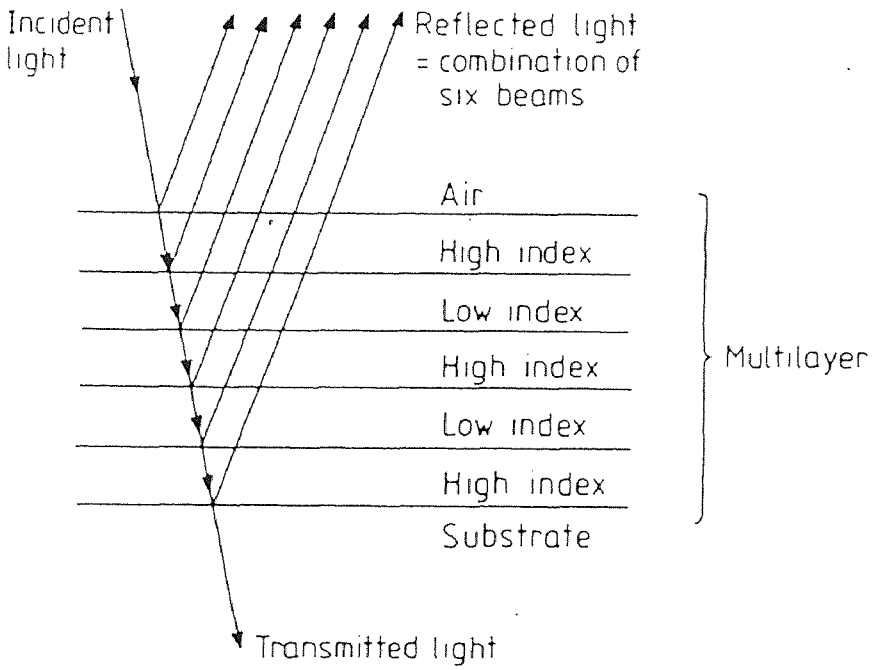

Figure 2.1 A multilayer of quarter wavelength thick films.

produced by reflection at successive boundaries throughout the assembly will appear at the front surface with all in phase so that they will recombine constructively. This is the basic form of high-reflectance coating. When such a coating is constructed, it is found that the reflectance remains high over only a limited range of wavelengths, depending on the ratio between high and low refractive indices. Outside this zone, the reflectance changes abruptly to a low value. Because of this behaviour, the quarter-wave stack is used as a basic building block for many types of thin-film filters.

In a Fabry-Perot interferometer(Fig. 2.2), the stack is used as a reflector. The interferometer consists of a spacer layer which is usually half a wavelength thick, bounded by two high-reflectance coatings. Multiple-beam interference in the spacer layer causes the the transmission of the filter to be extremely high over a narrow band of wavelengths for which the spacer is a multiple of one half wavelength thick.

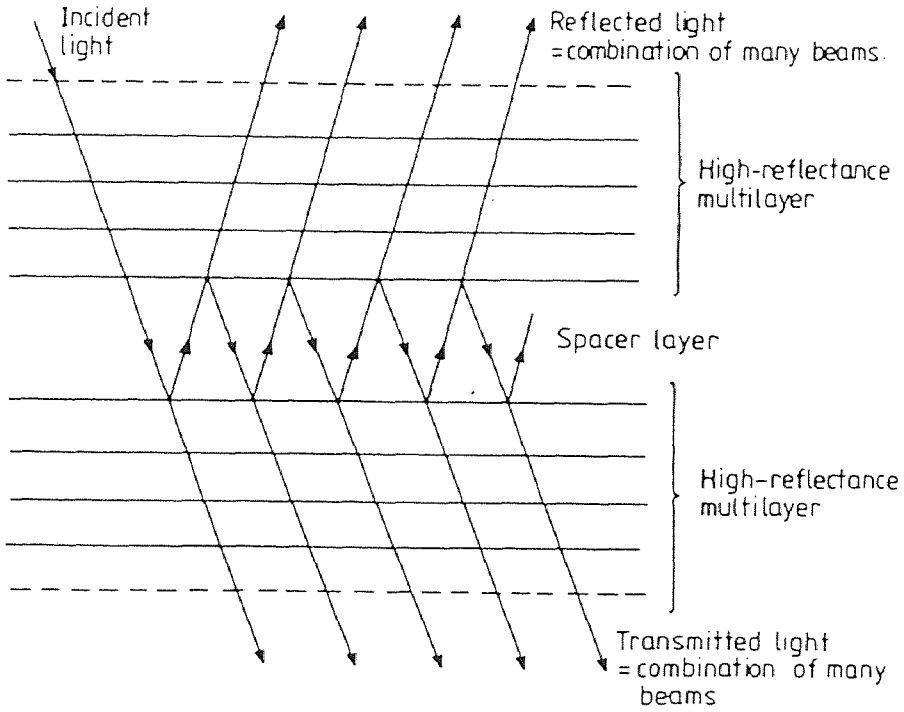

Figure 2.2 A Fabry-Perot filter showing multiple reflections in spacer layer.

2.2.1 Choice of Filter

A standard Fabry-Perot filter consists of dielectric spacer bound by two metal reflecting layers[10]. This provides a poor filter shape with low transmission and high absorption, but excellent rejection at wavelengths longer than the pass-band. If the metal is replaced by dielectric stacks, absorption can be minimized and transmission can be increased. However, the existence of long-wavelength transmission peaks can only be eliminated by additional dielectric stacks, vastly increasing the overall filter thickness and difficulty of manufacture. Since maximum transmission is not a requirement, an improved shape by some broadening of the filter pass-band will occur by stacking multiple filters to give a sequence Metal-Spacer-Metal-Spacer-Metal for a double half-wave filter. If the outer metal layers are replaced by dielectric stacks, absorption is reduced and transmission is increased, yet long-wave rejection is retained. The resulting D-S-M-S-D filter, as shown in Figure 2.3, is called an induced transmission filter. The dielectric-spacer combination (D-S) acts as an anti-reflection system for the metal at the peak wavelength, thereby increasing transmission.

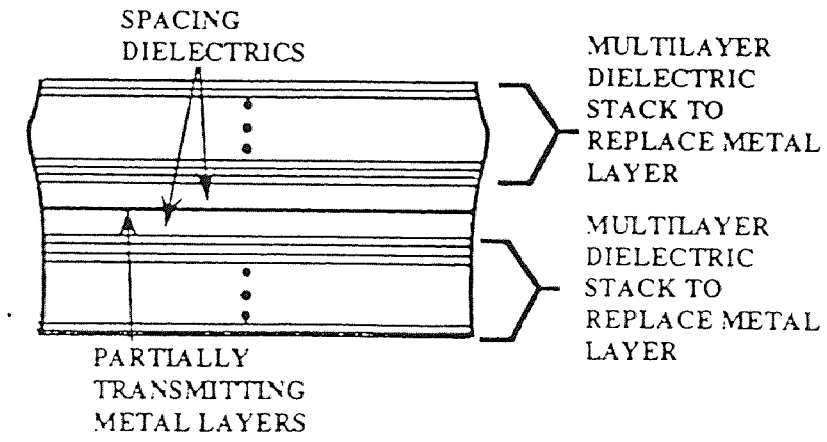

Figure 2.3 Induced transmission D-S-M-S-D Fabry-Perot filter.

This can be illustrated by a typical design, in this case, for 1.55 μm in Figure 2.4. Bandwidth at one-half peak transmission is 23 nm. Transmission above the pass-band is essentially zero, being between 0.01 and 0.1% over most of the range. Typically a total of 13 layers is required with a single silver layer at the center of the filter stack. To complete the filter, a long-wave pass glass absorption filter can be cemented to the induced transmission filter to remove any transmission below the pass-band.

To improve the rejection of the filter, it is necessary to have two metal layers with a dielectric layer between them. This will provide rejection of the order of 0.0001% at the expense of somewhat reduced transmission. Transmission may also be reduced and the peak narrowed by increasing the thickness of the metal layer.

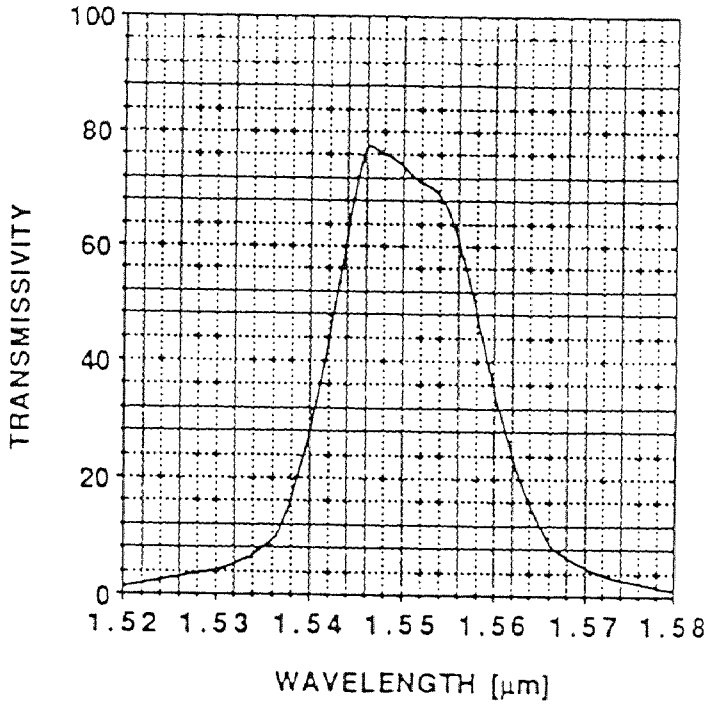

Figure 2.4 Calculated transmissivity in the pass-band vs. wavelength of a D-S-M-S-D filter with λ_0= 1.55 μm and $\Delta\lambda$= 23 nm.

2.3 Design Procedure

The thickness of the metal layer is very critical in filter design because the peak transmission is a function of this parameter. This is the basic problem tackled and solved by Berning and Turner[11]. The potential transmittance ψ of a layer or assembly of layers is defined as the ratio of the intensity leaving the rear surface to that actually entering at the front surface, and it represents the transmittance of the layer or assembly of layers if the reflectance of the front surface were reduced to zero. Thus, once the parameters of the metal layer are fixed, the potential transmittance is determined entirely by the admittance of the structure at the exit face of the layer. Furthermore it is possible to determine the particular admittance which gives maximum potential transmittance.

The design procedure is as follows: the optical constants of the metal layer at the peak wavelength are given. Then the metal layer thickness is chosen and the maximum transmittance together with the matching admittance at the exit face of the layer, which is required to produce that level of potential transmittance, is found. Often a minimum acceptable figure for the maximum potential transmission will exist and that will put an upper limit on the metal layer thickness. A dielectric assembly, which will give the correct matching admittance when deposited on the substrate, must then be designed. The filter is completed by the addition of a dielectric system to match the front surface of the resulting metal-dielectric assembly to the incident medium. The matching admittances for the metal layers are such that the dielectric stacks are efficient in matching over a limited region only, outside which their performance falls off rapidly, thus defining the limits of the pass-band of the filter.

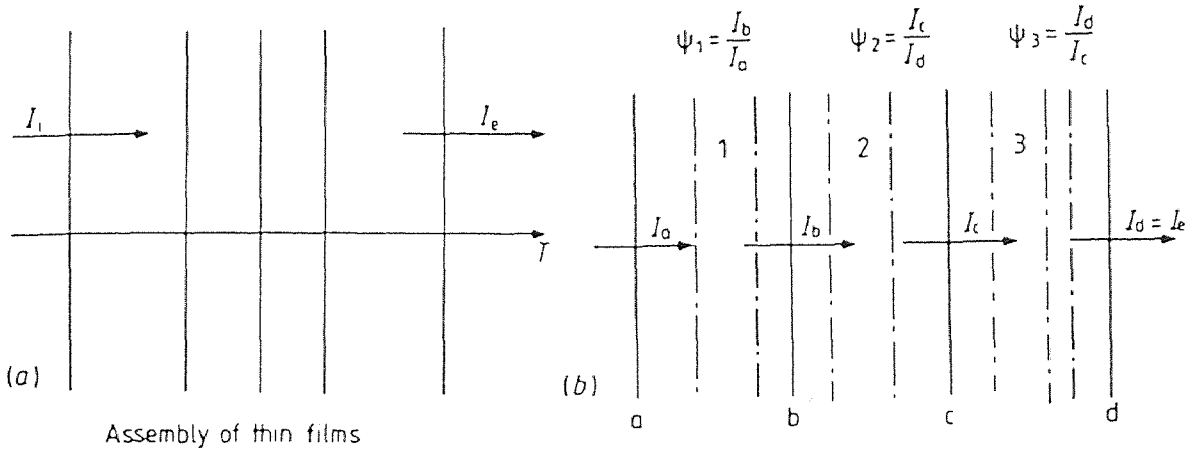

Figure 2.5 (a) An assembly of thin films. (b) The potential transmittance of an assembly of thin films consisting of a number of subunits.

2.3.1 Potential Transmittance

The analysis is limited to an assembly in which there is only one absorbing layer, the metal. The potential transmittance is related to the multilayer performance matrix for the assembly in Figure 2.5 by:

$$\begin{bmatrix} B_i' \\ C_i' \end{bmatrix} = [M] \begin{bmatrix} 1 \\ Y_e \end{bmatrix} \tag{2.2}$$

where, [M] is the characteristic matrix of the metal layer and Y_e is the admittance of the terminating structure. The potential transmittance ψ is given by

$$\psi = \frac{T}{(1-R)} = \frac{Re(Y_e)}{Re(B_i'C_i'^*)} \tag{2.3}$$

Let $Y_e = X + iZ$, then

$$\begin{bmatrix} B_i' \\ C_i' \end{bmatrix} = \begin{bmatrix} \cos\delta & (i\sin\delta)/y \\ iy\sin\delta & \cos\delta \end{bmatrix} \begin{bmatrix} 1 \\ X + iZ \end{bmatrix} \tag{2.4}$$

where $\delta = 2\pi(n - ik)d/\lambda = 2\pi nd/\lambda - i2\pi kd/\lambda$

$= \alpha - i\beta$

$\alpha = 2\pi nd/\lambda$

$\beta = 2\pi kd/\lambda$

If free space units are used, then $y = n - ik$

Now, $(B_iC_i^*) = [\cos\delta + i(\sin\delta/y)(X + iZ)][iy\sin\delta + \cos\delta(X + iZ)]^*$

$= [\cos\delta + i(\sin\delta/y)(X + iZ)][-iy^*\sin\delta^* + \cos\delta^*(X + iZ)]$ (2.5)

Taking the real part of Eqn. 2.5 and substituting it in Eqn. 2.3, the potential transmittance is

$$\psi = \left[\frac{(n^2 - k^2) - 2nk(Z/X)}{(n^2 + k^2)}(\sin^2\alpha\cosh^2\beta + \cos^2\alpha\sinh^2\beta)\right.$$
$$+(\cos^2\alpha\cosh^2\beta + \sin^2\alpha\sinh^2\beta)$$
$$+\frac{1}{X}(n\sinh\beta\cosh\beta + k\cos\alpha\sin\alpha)$$
$$\left.+\frac{X^2 + Z^2}{X(n^2 + k^2)}(n\sinh\beta\cosh\beta - k\cos\alpha\sin\alpha\right]^{-1} \qquad (2.6)$$

2.3.2 Optimum Exit Admittance

Next the optimum values of X and Z are calculated. From Eqn. 2.6

$$\frac{1}{\psi} = \left[\frac{q[n^2 - k^2 - 2nk(Z/X)]}{n^2 + k^2} + r + \frac{p}{X} + \frac{s(X^2 + Z^2)}{X(n^2 + k^2)}\right] \qquad (2.7)$$

where p,q,r, and s are symbols for the corresponding expressions in Eqn. 2.6. For an extremum in ψ, we have an extremum in $1/\psi$ and hence

$$\frac{\delta}{\delta X}\left(\frac{1}{\psi}\right) = 0 \qquad \text{and} \qquad \frac{\delta}{\delta Z}\left(\frac{1}{\psi}\right) = 0$$

$$\frac{q2nkZ}{X^2(n^2+k^2)} - \frac{p}{X^2} + \frac{s}{(n^2+k^2)} - \frac{sZ^2}{X^2(n^2+k^2)} = 0 \qquad (2.8)$$

and $$\frac{q(-2nkZ)}{X(n^2+k^2)} + \frac{2sZ}{X(n^2+k^2)} = 0 \qquad (2.9)$$

From Eqn. 2.9: $Z = nkq/s$

and, substituting in Eqn. 2.8,

$$X^2 = p(n^2+k^2)/s - n^2k^2q^2/s^2$$

Inserting the appropriate expressions for p, q, and s, from Eqn. 2.7,

$$X = \left[\frac{(n^2+k^2)(n\sinh\beta\cosh\beta + k\sin\alpha\cos\alpha)}{(n\sinh\beta\cosh\beta - k\sin\alpha\cos\alpha)} - \frac{n^2k^2(\sin^2\alpha\cosh^2\alpha + \cos^2\alpha\sinh^2\beta)^2}{(n\sinh\beta\cosh\beta - k\sin\alpha\cos\alpha)^2} \right]^{1/2} \qquad (2.10)$$

$$Z = \frac{nk(\sin^2\alpha\cosh^2\beta + \cos^2\alpha\sinh^2\beta)}{(n\sinh\beta\cosh\beta - k\sin\alpha\cos\alpha)} \qquad (2.11)$$

It can be noted that for large β, $X \to n$ and $Z \to k$, that is:

$$Y_e \to (n+ik) = (n-ik)^*$$

2.3.3 Maximum Potential Transmittance

The maximum potential transmittance can be found by substituting the values of X and Z, calculated by Eqns. 2.10 and 2.11, into Eqn. 2.6.

2.3.4 Matching Stack

Now an assembly of dielectric layers which, when deposited on the substrate, will have an equivalent admittance of

$$Y = X + iZ$$

This is illustrated diagramatically in Figure 2.6 where a substrate of admittance (n_s- k_s) has an assembly of dielectric layers terminating such that the final equivalent admittance is (X + iZ). Now the dielectric layer circles are always executed in a clockwise direction. If the diagram is reflected in the x-axis and then the direction of the arrows are reversed, identical set of circles are obtained - that is, the layer thicknesses are exactly the same - but the order is reversed (it was ABC and is now CBA) and they match a starting admittance of (X - iZ), i.e. the complex conjugate of (X + iZ), into a terminal admittance of (n_s+ ik_s), i.e. the complex conjugate of the substrate index.

There is an infinite number of possible solutions, but the simplest involves adding a dielectric layer to change the admittance (X - iZ) into a real value and then to add a series of quarter-waves to match the resultant real admittance into the substrate.

2.3.5 Front Surface Equivalent Admittance

If the admittance of the structure at the exit surface of the metal layer is the optimum value (X + iZ) given by Eqns. 2.10 and 2.11, then it can be shown that the equivalent admittance which is presented by the front surface is simply the complex conjugate of (X-iZ). The procedure for matching the front surface to the incident medium is therefore the same as that for the rear surface, so that the front dielectric section can be an exact repitition of the rear stack.

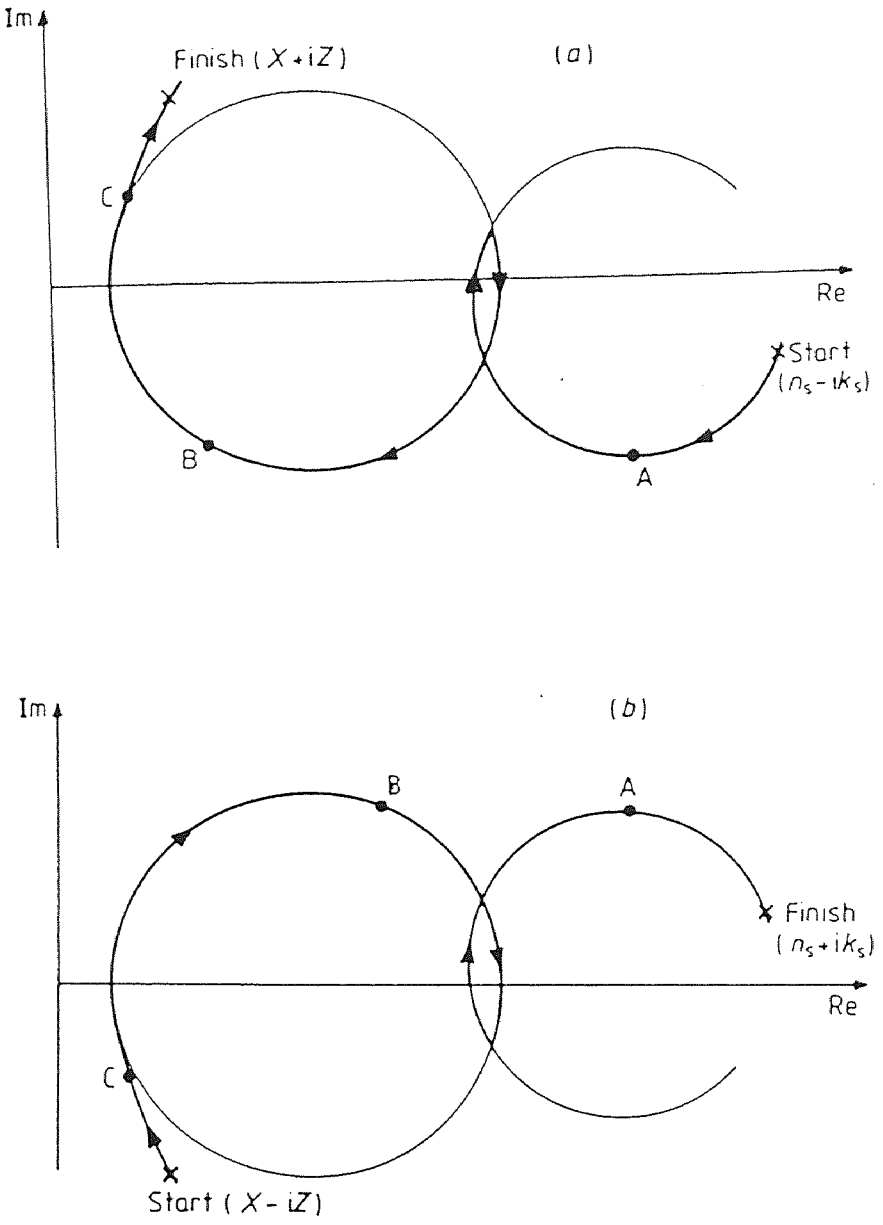

Figure 2.6 (a)A sketch of the admittance diagram of an arbitrary dielectric assembly of layers matching a starting admittance of (n_s-k_s) to the final admittance of (X+iZ).

(b)The curves of figure 2.5(a) reflected in the real axis and with the directions of the arrows reversed. This is now a multilayer identical to (a) but in the opposite order and connecting an admittance of (X-iZ).

2.4 Choice of Materials

There are several considerations for the choice of materials for the filter and the substrate. It is desirable that all materials provide a good match of the thermal coefficient of expansion, particularly as a quarter wave layer thickness of low index, for example, 1.55, required in a 4.5 μm filter is 0.7258 μm. Keeping the number of materials and layers to a minimum simplifies the deposition. As the sensor is made of silicon, it is the best material for substrate and the high index layer.

In order to minimize the number of layers required in the antireflection stacks, there should be a wide difference in the indices of refraction of the alternating high and low index layers. The choice of Si and SiO_2 or Al_2O_3 will accomplish this. The refractive indices of Si, SiO_2 and Al_2O_3 are 3.65, 1.55 and 1.59 respectively at 632.8 nm. Moreover, silicon suppresses any radiation below 1.1 μm.

A broader peak transmittance is obtained if the high index material is used as the spacer layers, but the thickness of those layers is about one-third of the low index spacers.

2.5 Filter Design

Once the materials are chosen for the filter, deposition parameters are set up for each material in order to achieve reproducibility in the optical characteristics. Then the optical constants, such as refractive index and extinction coefficient are determined by FTIR spectroscopy and these values are used as the design parameters. The filters were designed using the software developed by FTG software Associates. The performance of the filters depends on the optical characteristics of the materials.

2.5.1 Design Specification

The thickness of the dielectric stacks and spacer layers is fixed by the design wavelength of the filter. Each layer in the stack is quarter wavelength thick, while the spacer layer is half wavelength thick of the peak transmission wavelength. Thus, the metal layer thickness is of vital importance. The thickness of the metal layer can be arrived at by trial and error[3].

A filter was designed with center wavelength at 1.33 μm on silicon substrate using FILM*CALC 3.0. Silicon and Al_2O_3 has been taken as the high and low refractive index materials respectively, with Al_2O_3 as the spacer layers and Al as the metal. The effect of varying metal thickness on filter design has been simulated by using the program.

If the metal layer is less than optimum in thickness, the effect will be a broadening of the passband and a rise in peak transmission at the expense of an increase in background transmission remote from the peak. This can be seen in the broadband spectrum in Figure 2.7 for the filter with metal thicknesses of 0.02 and 0.03 μm. A splitting of the passband will also become noticable with the appearance of two seperate peaks eventually, if the thickness is further reduced.

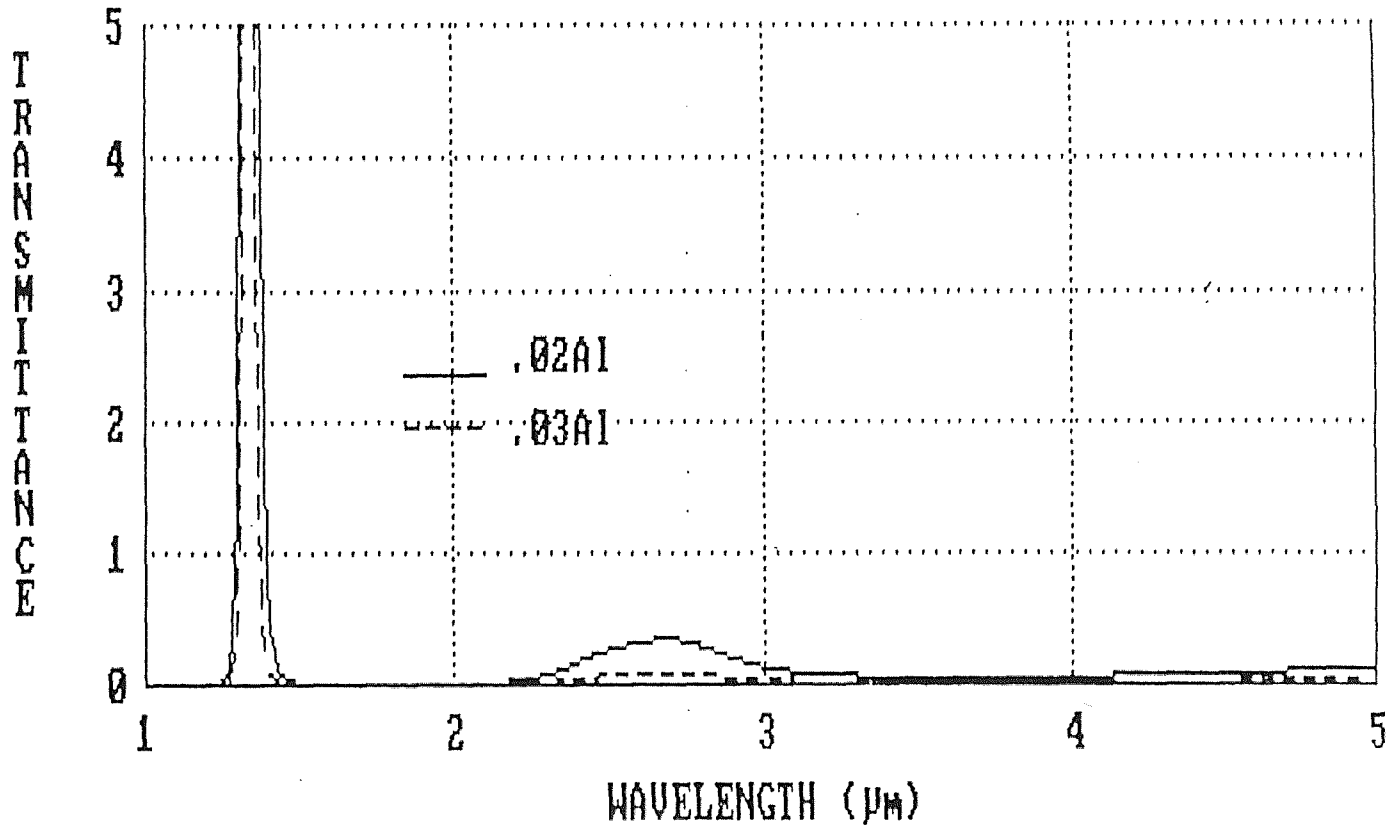

Figure 2.7 Rejection spectrum of filters using different metal thicknesses. Rejection improves with increasing metal thickness (in μm).

If the metal layer is made too thick, the effect will be a narrowing of the peak with a reduction of peak transmission. Figure 2.8 shows the performance of the filter for varying metal thicknesses of 0.02, 0.025, and 0.03 μm. It is clearly seen that the passband narrows and peak transmission decreases with increase in metal thickness.

The best results are usually obtained with a compromise in thickness where the peak is still single in shape but where any further reduction in metal thickness would cause the splitting to appear. As rejection is more important than maximum peak transmission, as required by the design specifications, the metal thickness was taken to be 0.03 μm. The broadband transmission in Figure 2.9 suggests excellent rejection with a peak transmission of 50%.

A filter with peak transmission at 1.5 μm was also designed with the metal layer 0.03 μm. The transmittance spectrum of the filter is given in Appendix I.

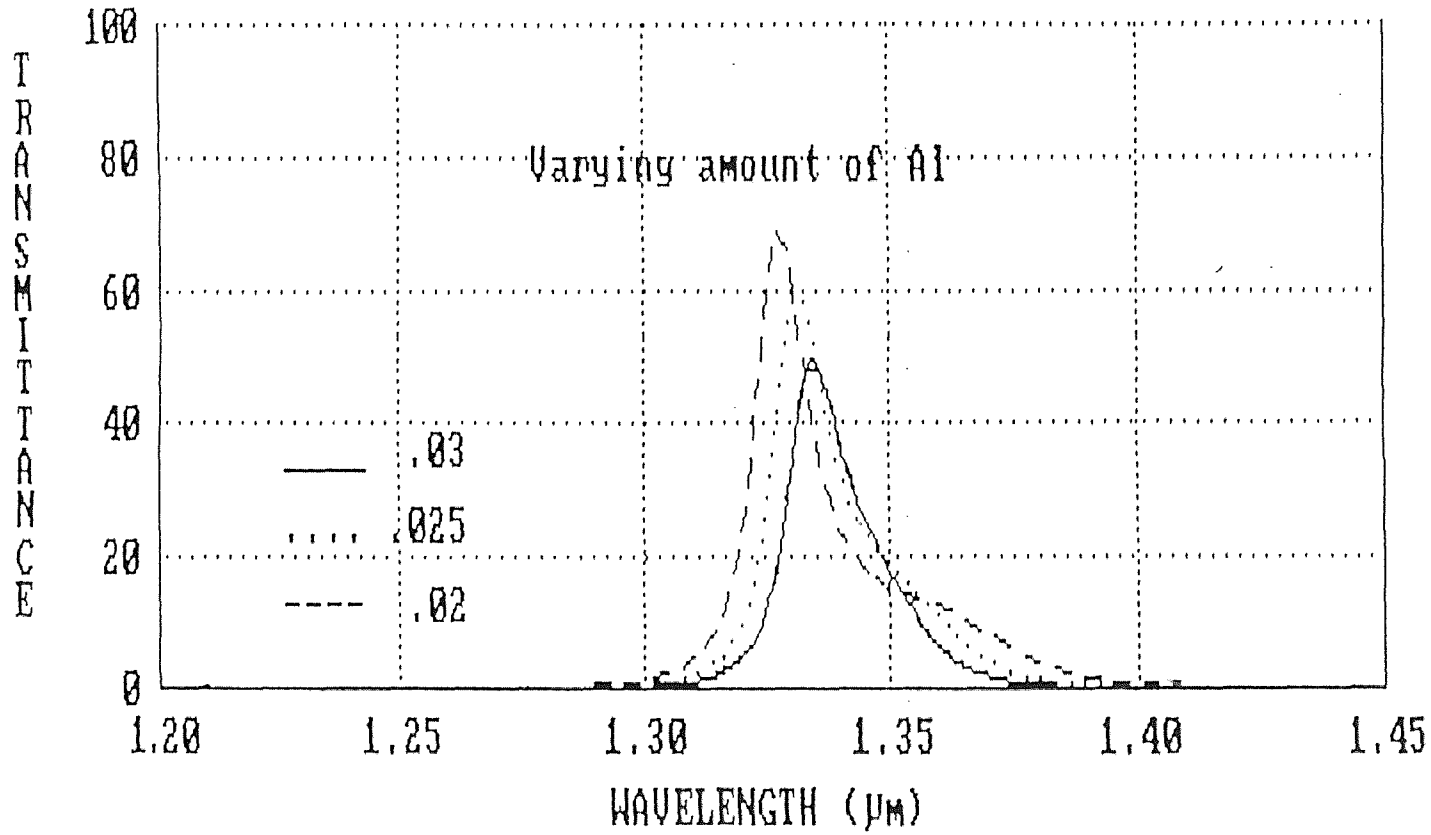

Figure 2.8 Dependence of filter design on metal thickness. Transmission decreases and passband narrows with increasing metal thickness (in μm).

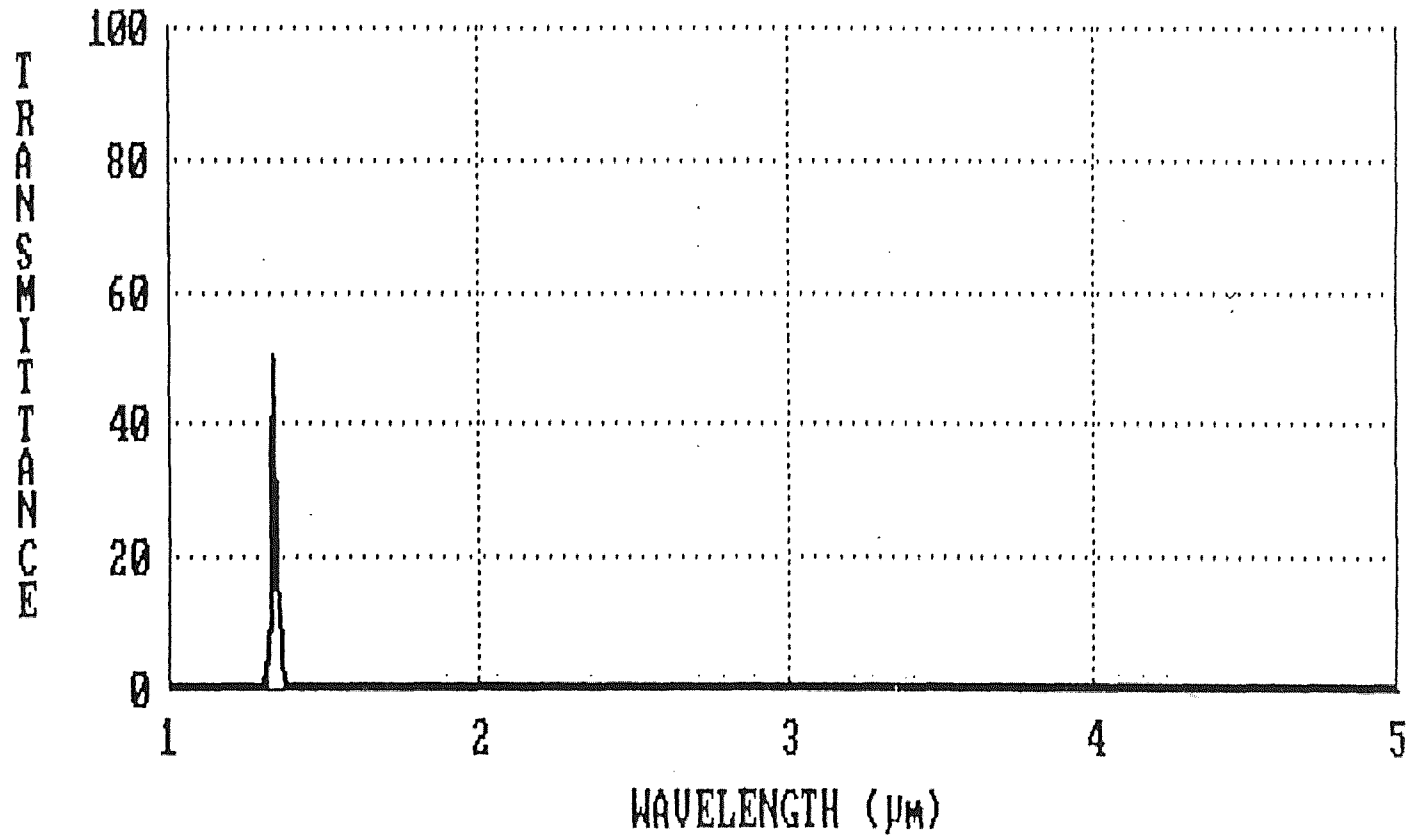

Figure 2.9 Broadband transmission curve showing the rejection spectrum for filter with peak transmission at 1.33 μm.

CHAPTER 3
THICKNESS MONITORING

3.1 Introduction

In the field of optical thin films, the accepted meaning of the term monitoring is the measurement and control of the parameters of optical thin films with the object of ensuring the deposition of an acceptable layer[12]. Monitoring, therefore, involves measurement, but the measurements must be made during deposition, and the results must be used to control the process and layer parameters.

The thickness of an individual film or of a series of many films represents a dimension which figures in practically all equations used to characterize thin films. Thin film thickness can be distinguished as physical thickness, mass thickness, and optical thickness. The physical thickness is defined as the step height between the substrate surface and the film surface. This step height multiplied by the refractive index of the film is termed as the optical thickness and is expressed generally in integer multiples of fractional parts of a desired wavelength. Finally, the mass thickness is defined as the film mass per unit area obtained by weighing. Knowing the density and optical data of a thin film, its mass thickness can be converted into the corresponding physical as well as optical thickness. Although film thickness has the dimensions of length, the measurement of it, obviously, cannot be accomplished with conventional methods for length determinations but requires special methods.

The main problem in controlling the deposition of layers is that the layers should have the characteristics required by the filter design. Many properties are desired, but refractive index and optical thickness are the most

important. There is no satisfactory method, at present, of measuring the refractive index of that portion of the film that is being deposited. Such measurements are made later but for closed loop process control, dynamic measurements are required. In normal practice, deposition parameters, that would affect refractive index, are controlled so that the index produced for any given material is consistent. Measurements are made of the index and the data obtained is used in the filter design. On the other hand, film thickness can be readily measured, therefore, easily controlled.

3.2 Thickness Monitoring Methods

There are many ways in which the thickness can be measured. Parameters such as mass, electrical resistance, optical density, reflectance, and transmittance have been used as variables to monitor thickness. Some of the techniques are as follows[13][14][15]:

- Interference methods
- Photometric Method
- Stylus methods
- Optical reflectance and transmittance measurements
- Oscillating quartz microbalance
- Electrical methods
- Gravimetry

It is also very important to measure and control the rate of deposition since film structure and properties are affected by the deposition rate to some extent. Ratemeters can usually be used for all film materials. This is a distinct advantage in multilayer deposition of metals and dielectrics. The simultaneous measurement of thickness and rate with one and the same measuring principle is certainly of advantage, as in having a thickness

monitoring system which can be actively integrated in an automatic process control. In this study, optical monitoring has been used for thickness measurement while quartz crystal microbalance controlled the growth rate for filter fabrication.

3.3 Optical Monitoring

Optical monitoring methods may be divided into two principal groups, direct monitoring, where the measurements for the control of layer thickness are made on the actual component which is to be produced, and indirect monitoring, where the measurements are made on a series of separate test plates[16]. To these principal groups, a sub-group may be added. This comprises of semi-direct monitoring, where, although the measurement is made on a separate test plate, the entire multilayer is controlled on the same plate, with the object that any build-up of errors should be similar to that occuring in the actual coatings. The filters are multilayers consisting of a series of quarter-wave and half-wave layers and are therefore suitable for control by turning value monitoring which consists of depositing material until a turning value of reflectance or transmittance is reached.

3.3.1 Turning Value Method

The conventional method of optical monitoring of quarter-wave layers during the process of depositing dielectric filters and mirrors is to measure the transmitted or reflected signal and to stop the deposition when the signal exhibits an extremum (the turning value method)[17].

This technique consists of measuring the effective transmission or reflection during the production of semi-transparent films[9]. If a transparent or slightly absorbing film is deposited on a transparent substrate, the optical

reflectance and transmittance of the film and substrate, measured at one wavelength, shows a cyclic behavior, with increasing film thickness due to interference effects. Reflectance is reduced or enhanced dependiing on the relative value of the indices of the film and substrate combination. The variations of reflectance or transmittance is similar to sine wave and the turning points correspond to those wavelengths for which the optical thickness of the film is an integral number of quarter wavelengths[18].

The variation of reflectance (at a single wavelength) for increasing film thickness is shown in Figure 3.1, where various curves corresponding to different values of film refractive index are shown, the substrate being glass.

For the case of film refractive index, n_f being less than the substrate refractive index, n_s ($n_f < n_s$), the reflectance will decrease initially reaching a minimum when the film optical thickness is equal to one quarterwave of the wavelength used for measurement. The reflectance will then increase, reaching substrate values when the optical thickness is a halfwave.

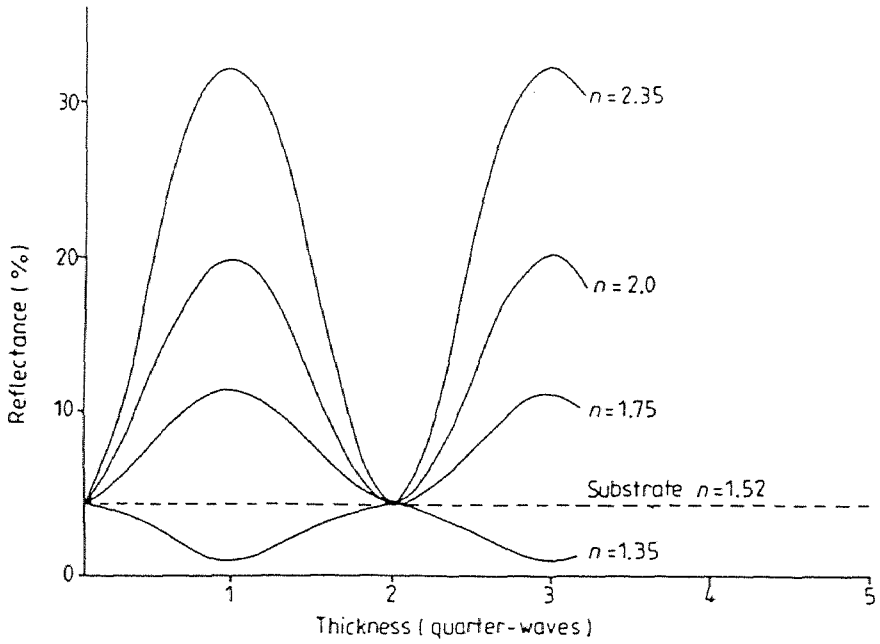

Figure 3.1 Calculated reflectance of single films on a single surface of glass.

For ($n_f < n_s$)

Reflectance minima occur at $nd = m\frac{\lambda}{4}$

Where, λ = wavelength of the light used for measurement

n = refractive index of the film

m = number of reflection or transmission peaks (odd integer)

d = physical thicness of depositing film

nd = optical thickness of depositing film

Reflectance maxima occur at $nd = (m+1)\frac{\lambda}{4}$

The position of maxima and minima is reversed if transmittance of the test piece is measured. The sequence of occurence is also reversed for $n_f > n_s$as compared with $n_f < n_s$.

The filter consists of a sequence of quarterwaves, or exact multiple of quarterwaves, of just two materials of high and low index. For such filters, it is sufficient to use as monitoring wavelength that wavelength for which the layers are quarterwaves, i,e. the peak transmission wavelength of the filter. The monitoring signal then displays a sequence of extrema, each corresponding to a further quarterwave optical thickness, and the layers are terminated at the appropriate extremum. The signal sequence is easily predictable, with almost no need for any calculation whatsoever or even any precise idea of the actual refractive indices.

3.3.2 Advantages of Turning Value Method

Layer thickness tolerance is very important in optical monitoring since, in a multilayer, the presence of an error in one layer can alter the effects of errors in all the other layers to an extent that is extremely difficult to predict

analytically in any meaningful way. Typical tolerance found by computerized Monte Carlo Techniques for narrowband filters is about half the fractional halfwidth[19]. Studies have indicated that, for narrowband filters, there is an enormous advantage in controlling all the layers in succession on the actual component that is to be produced. Because of error compensation, i.e. errors that can be caused by variations in the condensation behavior of the film material, turning value monitoring, instead of leading to large errors, yields filters with a high performance even in the presence of significant overshoots or undershoots of the desired termination points.

The immense success of the turning value monitoring method for narrowband filter production can be ascribed to the fact that high performance is required over a very limited wavelength range and the monitoring signal at one single wavelength is therefore a reasonable assessment of overall performance.

3.4 Quartz Crystal Microbalance (QCM)

The deposition of noble metal onto oscillating quartz crystals of the thickness shear type, for fine adjustment of their frequency, has been very popular with frequency standard manufacturers. The idea of using the frequency decrease by mass deposition to determine the weight of the coating was introduced by Saurbrey[20] and Lostis[21].

The normal modes of mechanical vibration of a quartz crystal have very high Q and can be transformed into electrical signals by the piezoelectric properties of quartz and viceversa[3]. The crystal acts as a very efficient tuned circuit that can be coupled into an electrical oscillator by adding appropriate electrodes. Any disturbances in its mechanical properties will cause a change in its resonant frequency. Such a disturbance might lead to an

alteration of the temperature of the crystal or its mass. The principle of monitoring by the quartz crystal microbalance is to expose the crystal to the evaporant stream and to measure the change in frequency as the film deposits on its face and changes the total mass. The frequency shift is converted internally into a measure of film thickness using film constants fed in by the operator. Since the signal from the quartz crystal monitor changes in the same direction, it can be more simply used in automatic systems than optical systems.

The AT-cut crystal oscillating in a thickness shear mode is best suited for the quartz crystal microbalance. The thickness x_q of an infinite quartz plate is directly related to the wavelength λ of the continuous elastic transverse wave, the phase velocity v_q of that wave and the frequency ν_q (i.e. the period τ_q) of the oscillating crystal, as shown in Figure 3.2.

$$x_q = \frac{1}{2}\lambda = \frac{1}{2}\left(v_q / \nu_q\right) = \frac{1}{2} v_q \tau_q \qquad (3.1)$$

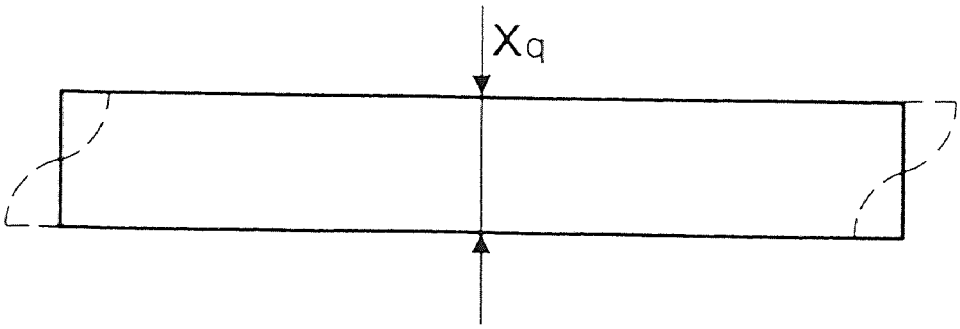

Figure 3.2 Schematic representation of a quartz crystal oscillating in the thickness shear mode (AT- or BT-cut).

By introducing the area density m_q of the quartz mass and the quartz density $\rho_q\left(m_q = \rho_q x_q\right)$, one obtains the exact relation between the relative frequency and the relative area mass density of the infinite thickness shear resonator:

$$\frac{d\nu_q}{\nu_q} = -\frac{dm_q}{m_q} \tag{3.2}$$

Changing to differences Δ results in

$$\frac{\Delta\nu_q}{\nu_q} = -\frac{\Delta m_q}{m_q} \tag{3.4}$$

Sauerbrey[20] substituted the area mass density Δm_q of an additional quartz wafer by the area mass density m_f of the deposited foreign material. He made the assumption that for small mass changes, the addition of foreign mass can be treated as an equivalent mass change of the quartz crystal itself. His relation for the frequency change of the loaded crystal is

$$\frac{\Delta\nu}{\nu} \cong -\frac{m_f}{m_q} \tag{3.5}$$

The restrictions of this formula are as follows:

(a) it is not mathematically rigorous;

(b) the elastic properties of the deposited material are different from those of the quartz crystal;

(c) the size of quartz crystal is finite;

Furthermore, the area exposed to deposition, i.e. the area covered by the electrodes, is different from that of the crystal. Nevertheless, this relation is well supported by experimental data up to a mass load of $m_f / m_q \leq 2\%$[22].

3.4.1 Disadvantages of Crystal Microbalance

The temperature dependence of the quartz frequency of the quartz resonator is a serious limiting factor in the resolution accuracy and reliability of measurements because it is not possible to protect detector crystals from the heat radiated by the evaporation source[23]. The use of water-cooled sensor heads decreases the area of the crystal surface exposed to the evaporation source, but the thermal lag between the crystal and the head and the inevitable temperature gradient between them reduces the effectiveness of the system, particularly as applied to the evaporation of very thin films.

The effect of intervening film layers on the measurement of thin-film thickness produces variations in measured thickness of typically less than 10%, but as much as 50% for some cases[24].

3.5 Comparison Between Turning Value Method and QCM

In spite of the considerable amount of work carried out on accuracy and tolerance in recent years, no clear answer has emerged as to the best system for monitoring, except perhaps in the case of narrowband filters where direct turning value optical monitoring gives best results[12].

Optical thickness is the most important parameter in the monitoring of deposition of optical thin films. For most coatings, optical thickness is the parameter with respect to which performance is most sensitive. Then there is relative ease in measuring optical thickness as compared with other parameters. Since refractive index measurement during deposition is extremely difficult, the monitoring of index as such is never attempted, and even the controlled deposition of mixtures to produce intermediate indices is carried out by making measurements of mass, i.e. by using quartz crystal monitor[25].

3.5 Optical Monitor Set-up

A typical arrangement to perform optical monitoring is shown in Figure 3.3. The arrangement provides for measuring the thickness of layers on optical elements during deposition, while coating all substrates equally. The use of modulated light eleminates interference from daylight and from light emitted by the evaporation source. The instrument has a monochromatic light source and can be operated in the visible and lower IR spectral range. For the intensity detection, visible and IR photodetectors are used. The use of two photodetectors arranged to detect reflected and transmitted light respectively, enables measurement of both intensities in rapid succession.

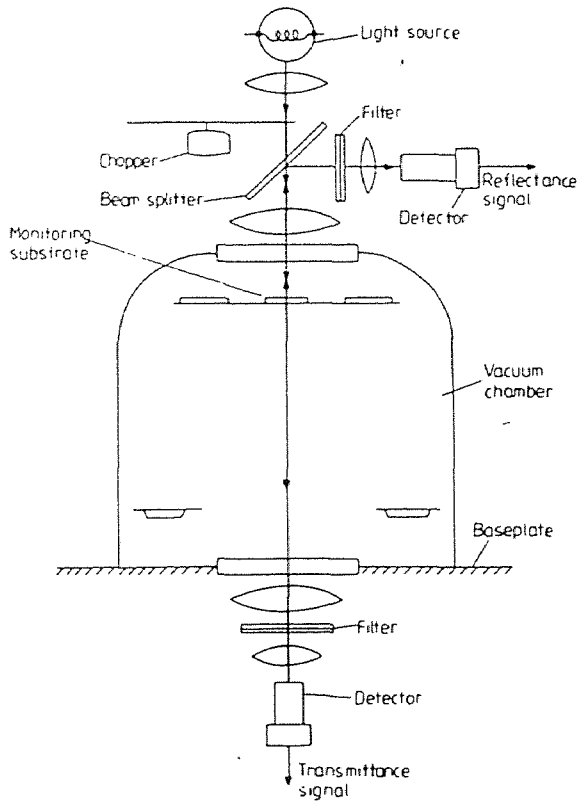

Figure 3.3 A possible arrangement of a monitoring system for reflectance and transmittance measurements.

Optical monitoring is carried out by projecting a light beam on the test piece being coated, and measuring the intensity of the reflected or transmitted light from the test piece. The beam of light, usually from an incandescent lamp, is chopped at some frequency and the signal is amplified at the chopped frequency to avoid noise and ambient light contributions to the detected signal and minimize zero drift problems. The light signal from the component being monitored is then made to enter the receiver unit where it is collected and made incident to the detector surface. Optical monitor is usually carried out at a single wavelength and thus the light beam is made to pass through a narrow bandpass filter or a monochromator before being incident on the detector surface. A monocromator is much more versatile than narrow band filters and permits monitoring over a wide wavelength range than a single wavelength. The narrow bandpass filter is usually more economic and compact.

For the visible range (300 to 900 nm), a silicon PIN photodiode is employed. This device, when properly used, is found to be linear over many decades of irradiance variation. For the infrared region (850 to 2500 nm), the PbS cell is commonly used.

The monitoring wavelength for the 1.5 μm peak transmission filter was set up at the same wavelength. The test piece used for monitoring the thicknesses of the depositing layers is glass, having a refractive index of 1.51. The first layer to be deposited is Al_2O_3 and it has a refractive index of 1.59. As the difference between the indices of the test piece and the depositing layer is very small, the change in the amplitude of the monitoring signal is also very small. This can be seen in Figure 3.4, which was simulated using the software FILM*CALC 3.0. This makes monitoring extremely difficult, because the turning point is not sharp and distinct.

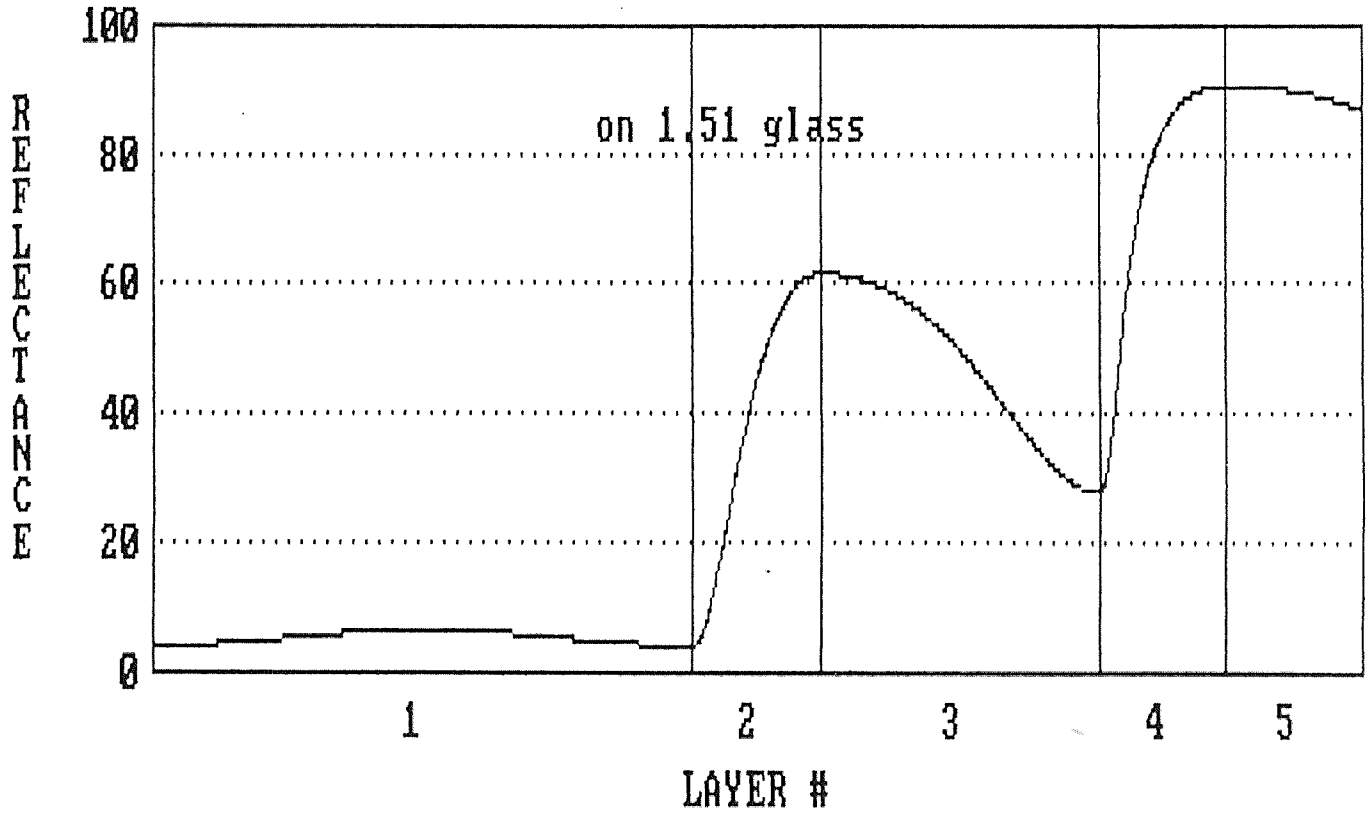

Figure 3.4 Optical monitoring curves for filter with peak transmission at 1.5 μm. The first layer deposited on the glass test piece is Al_2O_3 The monitoring signal for the first layer is very small. Monitoring wavelength is 1.5 μm.

This problem can be eliminated by depositing a quarter wavelength of silicon on the testpiece. The first layer on the test piece is then silicon, which has a high refractive index of 3.46. This method gives a sharp turning point when silicon is being deposited on glass and also when the second layer of Al_2O_3 is being deposited on silicon, thus making monitoring easy and accurate (Figure 3.5). The design of the filter does not change with the deposition of Si as the first layer, since the substrate is also Si.

It is very difficult to monitor the deposition of metal, i.e. aluminum, by the turning value method (Figure 3.6), since there is no distinct points to stop the deposition. As such, the deposition of Al is controlled by the quartz crystal monitor.

Filters were produced with the center wavelengths at 1.33 and 1.5 μm. Work, aimed at fabricating and characterizing filters, at 3.0 and 4.5 μm transmittance, is in progress. The monitoring of the deposition at the higher wavelengths may create some problems. The energy level at infrared is very small, and it gets smaller at higher wavelengths. Moreover, there is a drop of the monitoring signal at every stage of the device - fiber optics, monochromator, and filter. So, the monitoring of the deposition for the filters with peak transmission at 3.0 and 4.5 μm are carried out at the 1.5 μm, since both the wavelengths are a multiple of 1.5 μm. The monitoring curves for these filters are shown in Appendix IV. For the 4.5 μm filter, two test pieces are used to monitor the deposition.

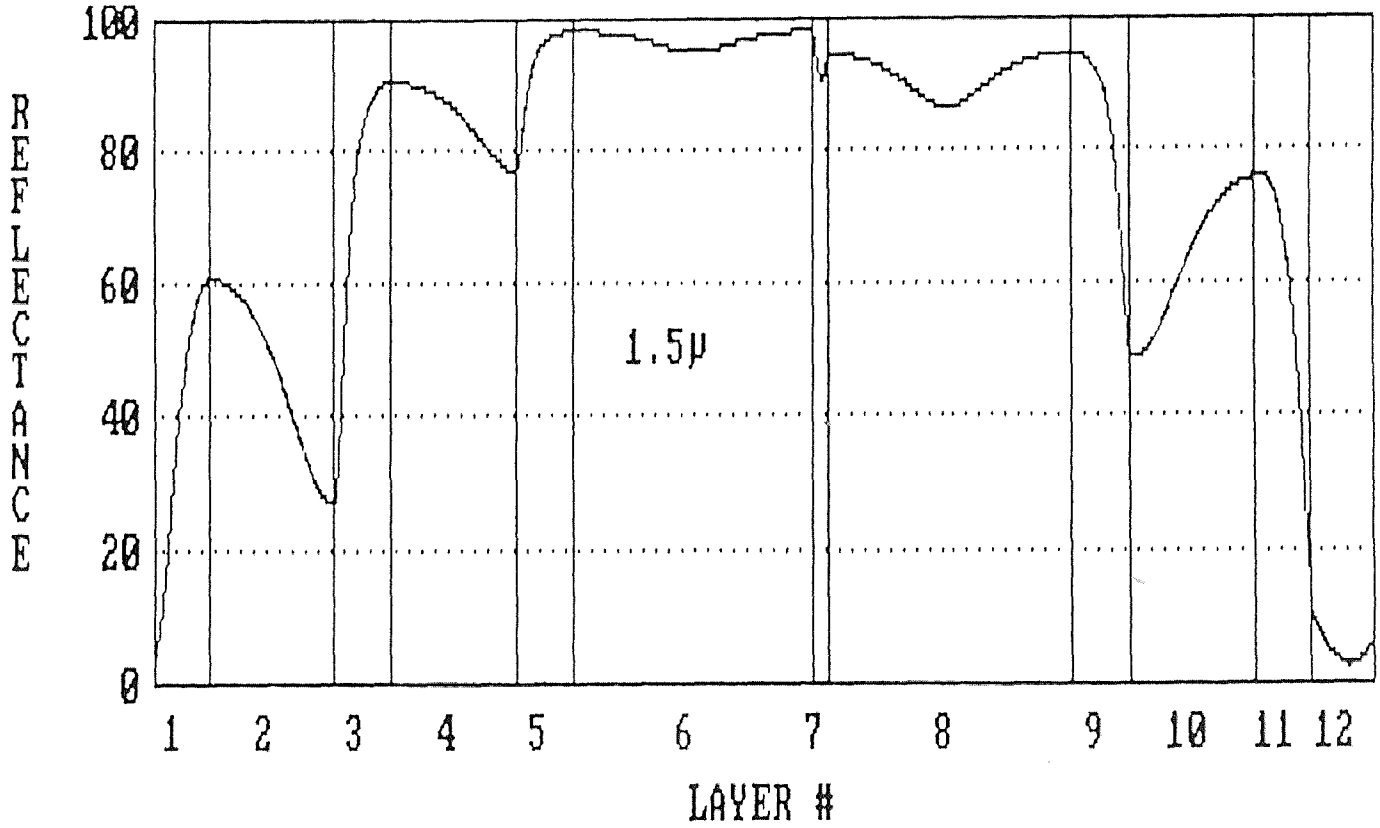

Figure 3.5 A quarterwave coating of silicon (Layer 1) was deposited on the glass test piece. An improvement in the monitoring signal for Al_2O_3 layer (Layer 2) is easily noticeable. Monitoring wavelength is 1.5 μm.

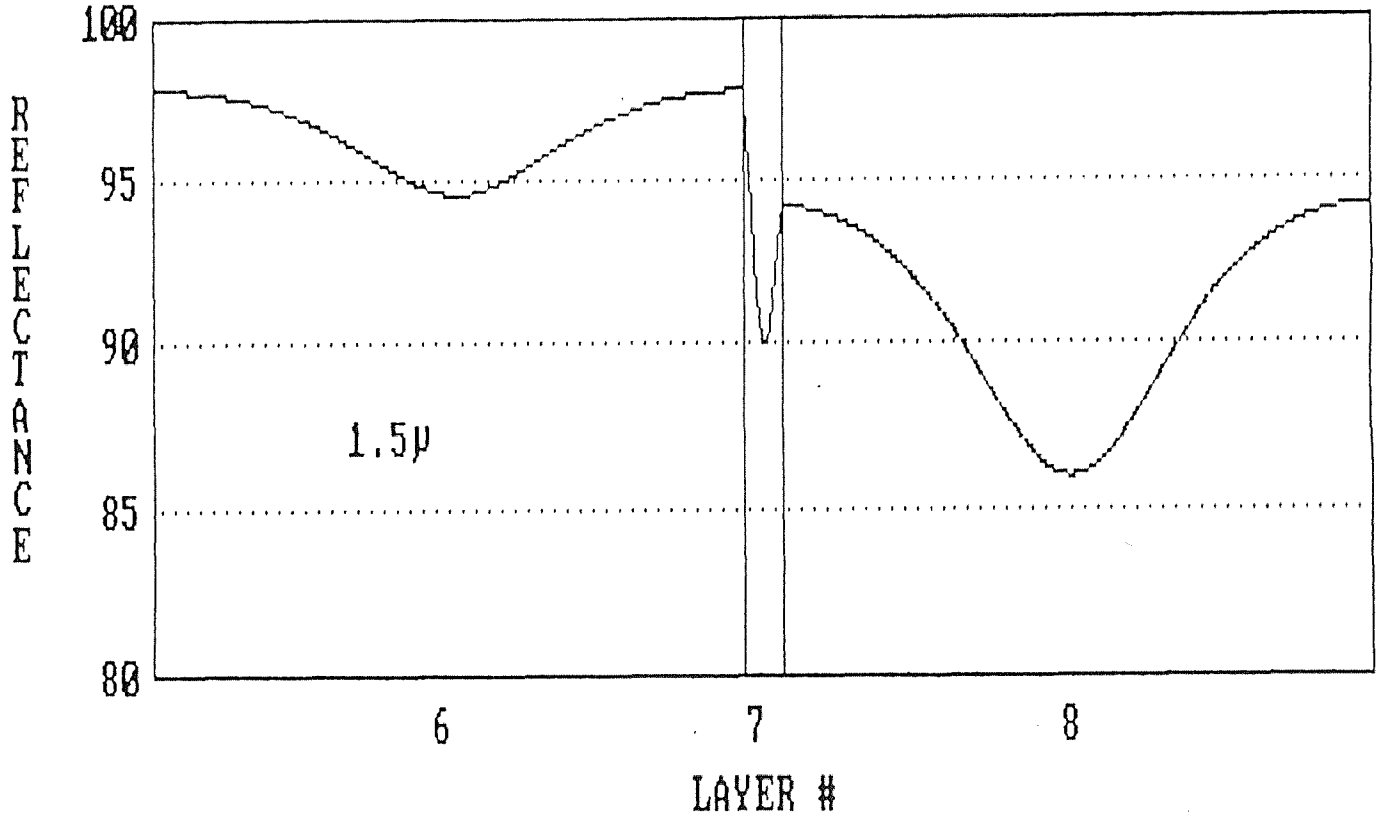

Figure 3.6 Detection signal for aluminum deposition. Layer 7 is aluminum.

CHAPTER 4
STUDY OF MATERIALS

4.1 Introduction

The relevance of traditional standards poses difficult questions when infrared materials are considered[26]. The well-tried and tested common glasses universally employed in the visible region of the spectrum are no longer of use in the infrared. There are no infrared materials so easily available, and therefore as cheap, or so easily worked on glass. Each optical component in the infrared must be considered in terms of a number of characteristics for the various possible materials. For example:

a) Optical properties such as refractive index and region of transparency.

b) The method to be used for the production of the material in thin-film form.

c) Mechanical properties of thin films such as hardness or resistance to abrasion, and the magnitude of any built-in stresses.

d) Chemical properties such as solubility and resistance to attack by the atmosphere, and the compatibility with other materials.

e) Toxicity.

f) Price and availability.

g) Other properties which may be important in particular applications such as electrical conductivity or dielectric constant.

There are several considerations entering into the choice of materials for the filter and the substrate. Si and SiO_2 or Al_2O_3 were considered as the high and low refractive index materials, with Al being the metal. The dielectric materials were selected since there is a considerable difference between the indices, thus keeping the number of layers of the filter to a minimum and the fabrication process simple. Al_2O_3 was taken as the spacer

layer for the filter. Si acts as a natural cutoff filter design in the lower wavelength for the desired design. Al was the metal of choice because of its availability, ease of deposition, and compatibility with silicon processes. All the materials chosen provide a good match of the thermal expansion. Fourier Transform infrared (FTIR) spectroscopy was performed on each of the samples to obtain the optical constants of the materials and use these values for the filter design.

4.2 Fourier Transform Infrared Spectroscopy

As the name implies, FT spectroscopy involves a special mathematical treament of spectral data[27]. FT spectroscopy of infrared radiation has two major advantages over the conventional dispersive instruments. First, infrared spectra can be recorded at a much greater speed or at a greater sensitivity than can be achieved with a dispersive spectrometer. Second, the spectrum is measured at a constant resolution over the entire spectral region with FTIR spectrometers, as opposed to a grating instrument in which the resolution varies with frequency.

4.2.1 Theoretical Background

A blackbody is defined as an object which absorbs all of the light falling on it[28]. When heated, a blackbody emits radiation with a frequency distribution which depends only on the temperature of the body, i.e. the distribution of emitted energy is independent of the material from which it is constructed. Planck's law formulates the distribution of energy emitted by a blackbody as a function of absolute temperature:

$$\rho(\nu,T) = \left(8\pi h\nu^3 / c^3\right)\left[\exp(h\nu / kT) - 1\right]^{-1} \qquad (4.1)$$

where $\rho(\nu,T)$ is the density of radiation of frequency ν at temperature T. Planck's radiation law is important because it correctly predicts the distribution of energy emitted from a blackbody for any frequency at a given temperature. Several examples of blackbody radiation curves calculated from Eqn. (4.1) are shown in Figure 4.1. The frequencies are given in cm^{-1}, but $\rho(\nu,T)$ has the units of erg/cm^3sec^{-1}, i.e, energy density per unit of frequency in sec^{-1}. It can be seen from the figure that the peak value of ρ increases and shifts to higher frequencies with increasing temperature. The total energy density within a blackbody cavity can be found by integrating Eqn. (4.1) over the frequency interval $(0, \alpha)$. The result is given by

$$\int_0^\infty \rho(\nu,T)d\nu = \left(8\pi^5 k^4 / 15c^3h^3\right)T^4 \qquad (4.2)$$

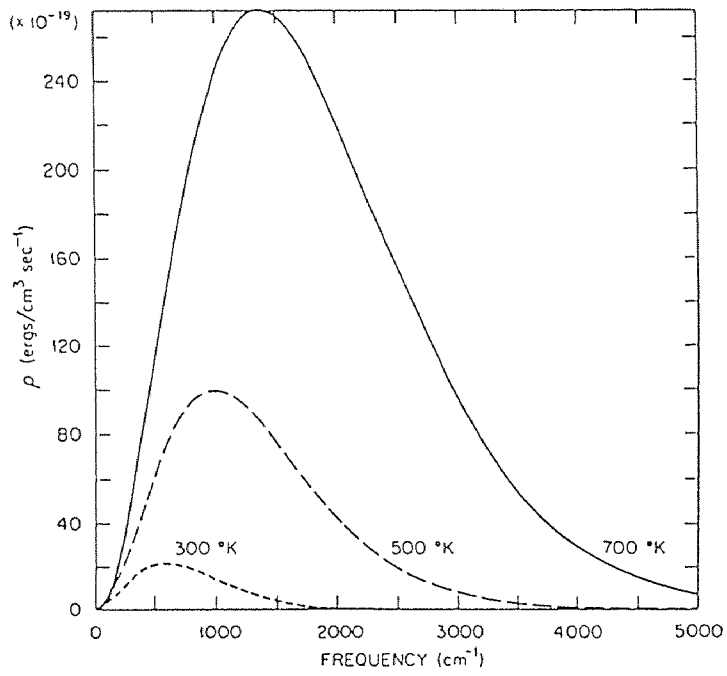

Figure 4.1 Graphs of Planck's blackbody radiation function for different temperatures.

Eqn. (4.2) may be compared to the Stefan-Boltzman law, which is expressed by $\rho = \text{constant} \times T^4$. The value of ν for which ρ is a maximum at a given temperature can be found from $d\rho / d\nu = 0$. Denoting this value of ν by ν_m, it is found that

$$\frac{\nu_m}{T} = \ln\left(\frac{3}{3 - h\nu_m / kT}\right)\frac{k}{h} \tag{4.3}$$

A graphical solution of Eqn. (4.3) shows that $\nu_m / T \cong 1.93$ cm^{-1}/deg., or $\nu_m = \text{constant} \times T^4$. This is Wein's law, which states that ν_m increases in proportion to the absolute temperature. Thus, Planck's law is consistent with the earlier empirical laws of blackbody radiation.

Since blackbody radiation does not depend on the composition of the radiator, it does not provide any spectral information about the material. However, materials in general are nonblack radiators, and the emission from a gas at low pressures, for example, contains discrete spectral lines which are characteristic of the constituents of the gas. an expression for the distribution of radiation from a nonblack or graybody may be obtained by using Kirchoff's and Planck's radiation laws[29]. The spectral emissivity of a graybody at a temperature T, ε_ν, is defined as the ratio of the spectral radiance or radiant flux, $J(\nu,T)$, to that of a blackbody at the same temperature, $J_B(\nu,T)$:

$$\varepsilon_\nu = \frac{J(\nu,T)}{J_B(\nu,T)} \tag{4.4}$$

Kirchoff's law states that $\varepsilon_\nu = \alpha_\nu$, where α_ν is the spectral absorptivity. In order to derive an expression for the emissivity of a semitransparent material, only the radiation travelling normal to the emitting surface is considered. For the emission from a plane parallel layer located at a distance X from the front surface of a semitransparent slab of total thickness d, if $j(\nu,T)$ is the spectral

emissive power of this layer at temperature T, then radiation received at the front surface is

$$j(\nu,T,X) = j(\nu,T)\exp\left[-k(\nu,T)X\right] \tag{4.5}$$

where, $k(\nu,T)$ is the absorption coefficient. If the reflectivity is denoted by $r(\nu,T)$, then the radiation emerging out of the surface from the layer at X is

$$j(\nu,T,X) = \left[1 - r(\nu,T)\right]j(\nu,T)\exp\left[-k(\nu,T)X\right] \tag{4.6}$$

The fraction of radiation which is reflected back into the body is rj[exp(-kX)], and after traversing the distance d, arrives at the back surface with intensity attenuated by the amount exp(-kX). By definition, $t(\nu,T) = \exp\left[-k(\nu,T)d\right]$ is the transmissivity of the material at frequency ν and temperature T. Thus the intensity of radiation reaching the back surface is given by rtj[exp(-kX)]. The repeated process of reflection and transmission is illustrated in Figure 4.2. The arrow starting at A represents the path of a ray emitted from the layer at X toward the front surface of the slab, and the arrow starting at point B represents the path of a ray emitted from X toward the back surface.

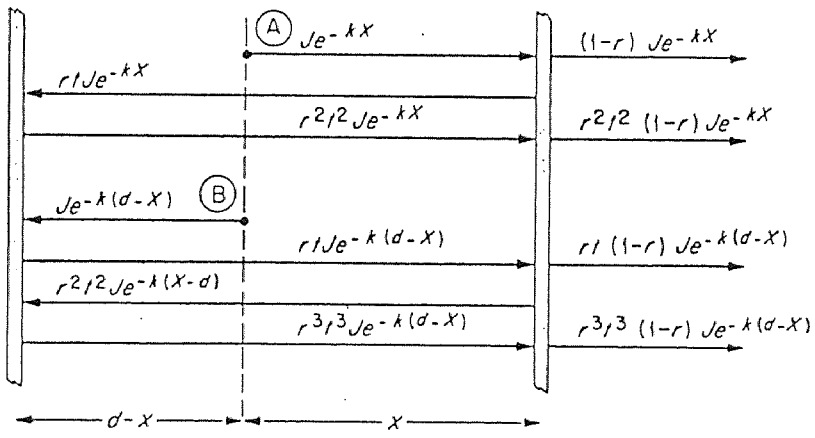

Figure 4.2 Schematic representation of emission from a semi-transparent material.

Although the ray starting at A or B retraces the same path on successive reflections, these events are represented by seperate arrows, which are displaced downward along the vertical axis of the slab. The expression at the tip of each arrow is the radiancy at that point. It can be seen from the figure that the total radiation emerging out of the front surface as a result of emission toward the front surface from the layer at X (ray at A) is given by

$$\sum_{n=1}^{\infty} r^{2n-2} t^{2n-2} (1-r) j(\nu,T) \exp(-kX) \tag{4.7}$$

The radiation emitting from the layer at X towards the back surface contributes to the total radiation emerging out of the front surface. The total contribution from this back emission from the layer is given by

$$\sum_{n=1}^{\infty} r^{2n-1} t^{2n-1} (1-r) j(\nu,T) \exp\left[-k(d-X)\right] \tag{4.8}$$

The total emissivity at frequency ν and temperature T, emerging out of the front surface of the semitransparent slab, is given by the sum of eqns. (4.7) and (4.8), in which the exponential terms must be integrated between the limits of 0 and d. Thus,

$$J(\nu,T) = \sum_{n=1}^{\infty} \left\{ r^{2n-2} t^{2n-2} (1-r) j(\nu,T) \int_0^d \exp(-kX) dX \right\}$$

$$+ \sum_{n=1}^{\infty} \left\{ r^{2n-1} t^{2n-1} (1-r) j(\nu,T) \int_0^d \exp\left[-k(d-X)\right] \right\} \tag{4.9}$$

Performing the integrations and collecting the terms gives

$$J(\nu,T) = (1-r)(1-t) \frac{j(\nu,T)}{k(\nu,T)} \sum_{n=0}^{\infty} r^n t^n \tag{4.10}$$

The integration of both terms of eqn. (4.9) gives [1-exp(-kd)] = 1-t. Since $r < 1$ and $t < 1$, the infinite series of eqn. (4.10) converges to $(1 - rt)^{-1}$, and, therefore,

$$J(\nu,T) = \frac{(1-r)(1-t)}{(1-rt)} \frac{j(\nu,T)}{k(\nu,T)} \tag{4.11}$$

If either r = 0 or t = 0, Kirchoff's law can be applied to eqn. (4.11) in order to identify the yet undefined quantity $j(\nu,T)$. If r = 0, then

$$J(\nu,T) = (1-t)\frac{j(\nu,T)}{k(\nu,T)} \tag{4.12}$$

From the statement of Kirchoff's law in eqn. (4.3), $\alpha_\nu = 1 - t = \varepsilon_\nu$, and since $\varepsilon_\nu = J / J_B$, it follows that $J_B = j(\nu,T) / k(\nu,T)$. McMahon[30] defines $j(\nu,T)$ as the volume spectral emissive power and finds $j(\nu,t) / k(\nu,t) = 2J_B$, while from Gardon's[31] more detailed treatment, $j(\nu,t) / k(\nu,t) = \left(n^2 / \pi\right)J_B$, where n is the refractive index. The definition of j in both cases depends on the solid angle chosen for the blackbody radiation. Inserting the result $J_B = j / k$ into eqn (4.11) produces the expression for the radiancy of a semitransparent material:

$$J(\nu,T) = \frac{(1-r)(1-t)}{(1-rt)} J_B \tag{4.13}$$

From eqn (4.4), the emissivity is given by

$$\varepsilon(\nu,T) = \frac{(1-r)(1-t)}{(1-rt)} \tag{4.14}$$

where, reflectivity, r and transmissivity, t are functions of the wavelength ν and temperature T. By multiplying both sides of eqn (4.14) by (1 - rt),

$$\varepsilon + r + t = 1 + \varepsilon rt + rt \tag{4.15}$$

The second and third terms of the right-hand side of eqn. (4.15) are small and can be neglected. Thus an extended Kirchoff's law is obtained by

$$\varepsilon + r + t \cong 1 \tag{4.16}$$

4.2.2 General Experimental Procedures

The measurement of infrared emission spectra usually requires special sampling techniques and equipment which depend on the nature of the emitting source. The procedure of obtaining the emissivity of a sample is described mathematically by eqn. (4.4). The value of the spectral radiancy of a sample at temperature T and frequency ν is divided by the radiancy of a blackbody at the same temperature and frequency. The emission spectrum of the sample at temperature T is given by the graph of ε_ν vs ν. If the instrument resolution is given by $\Delta\nu$, then spectral radiancy of the sample and blackbody will be given by $J(\Delta\nu,T)$ and $J_B(\Delta\nu,T)$, respectively. $J(\Delta\nu,T)$ may be very small, so the throughput and multiplex advantages gained by using interferometric rather than dispersive techniques are important and often essential in emission spectroscopy.

The measurement of quantitative emissivities or emission spectra requires a determination of $J_B(\Delta\nu,T)$, the radiancy of an ideal blackbody. The emission from a hole drilled in a cylindrical piece of material which is held at constant temperature is nearly as efficient as the emission from an ideal body. The efficiency is determined by the ratio of the length of the hole to its radius and by the emissivity of the material. The main problem arises in measuring only the radiation from the hole and excluding that from the surrounding wall[32]. Simpler and more practical blackbody sources have been reported. An example of a heated sample cell which includes a blackbody reference is shown in figure 4.3[33].

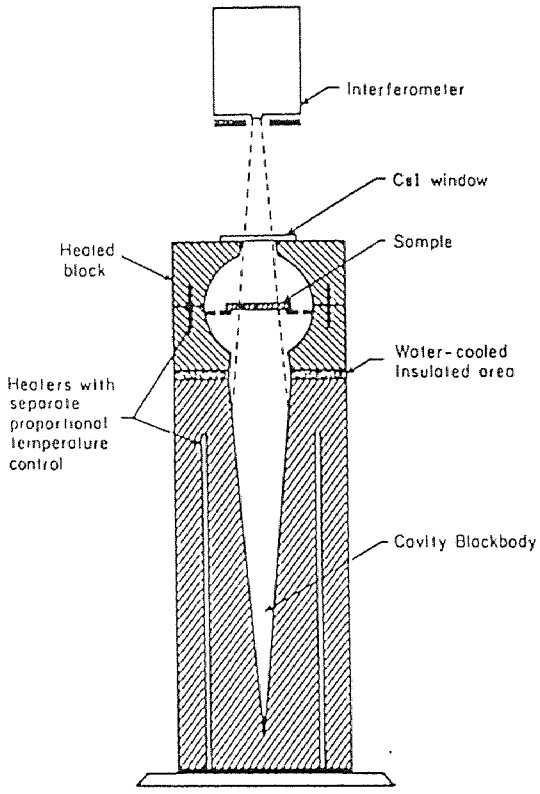

Figure 4.3 Schematic of an IR emission furnace with a blackbody reference.

4.3 Silicon (Si)

All semiconductors exhibit a sudden transition from opacity to transparency at a certain wavelength known as the intrinsic edge. This wavelength corresponds to the energy gap between the filled valence band of electrons and the empty conduction band. For Si, this wavelength is 1.1 μm. At wavelengths shorter than this photons are absorbed in the material because they are able to transfer their energy to the electrons in the filled valence band by lifting them into the empty conduction band[34]. At wavewlengths longer than this value, the photon energy is not sufficient, and apart from a little free-carrier absorption, there is no mechanism for absorbing the energy. The material appears transparent until lattice vibration bands at rather long wavelengths.

The optical properties of amorphous silicon (a-Si) are sensitive to preparation conditions and to doping with hydrogen[35].The optical properties of a-Si are also affected by the amount of disorder in the samples. Disorder is determined by substrate temperature, deposition rate, deposition method, impurities, vacuum conditions, annealing conditions, and environmental conditions. The mismatch of the expansion coefficient of the sample and the substrate introduces stress that can cause grain boundaries and voids in the sample. Annealing of the samples will reduce the strain but will generally increase the surface roughness.

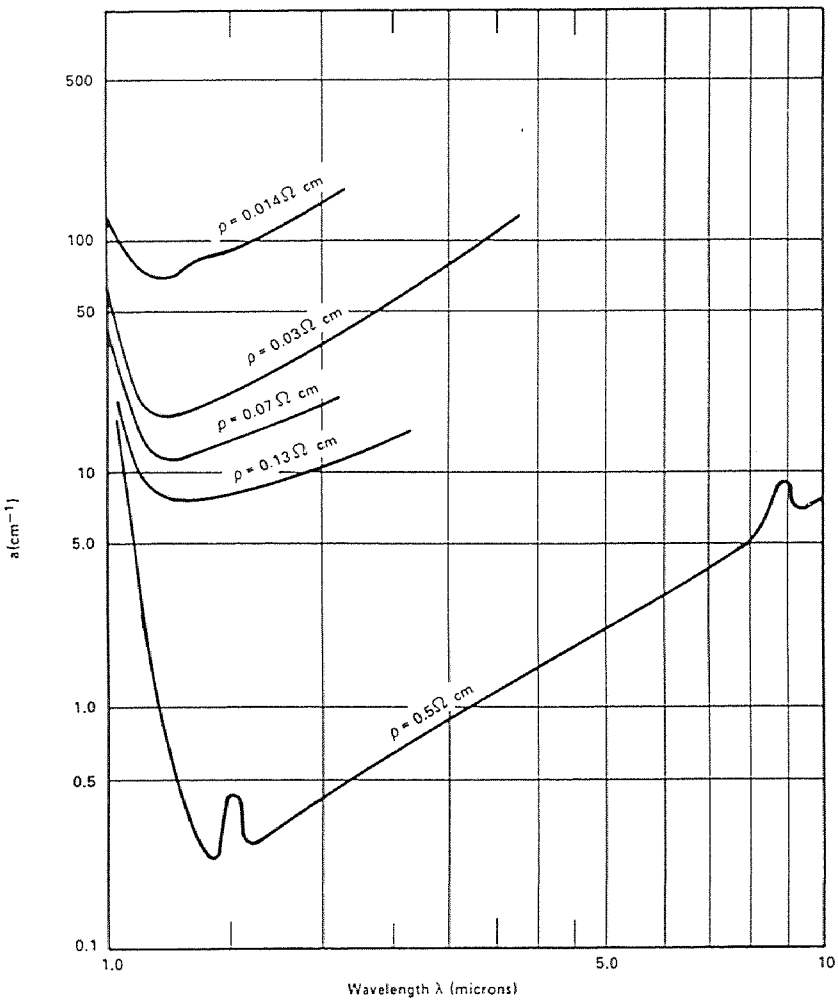

Figure 4.4 Absorption coefficient of p-type Si as a function of wavelength.

Silicon is fairly transparent in the infrared region beyond 1.1 μm. A study of the absorption coefficient as a function of wavelength for different temperatures (Figure 4.4) show that transmission is best at lower temperatures[36]. At 77°K, the absorption coefficient is about 12 cm^{-1} at a wavelength of 1.1 μm rising to 40 cm^{-1} at 2.2 μm. At 663°K, the absorption has a minimum value of about 37 cm^{-1} at a wavelength of 1.35 μm and rises to a value of over 70 cm^{-1} at 2.3 μm. The infrared transmission of silicon varies with purity and the study was performed on a Si sample with a resistivity of only 0.03 Ω-cm. The transmission of pure silicon shows fairly uniform transmission from 2 μm to the limit of measurements of 22 μm (Figure 4.5).

Silicon is not at all easy to evaporate because it reacts strongly with any crucible material, and the only way of dealing with this is to use an electron gun with a water-cooled crucible so that the cold silicon in contact with the crucible wall acts as its own container.

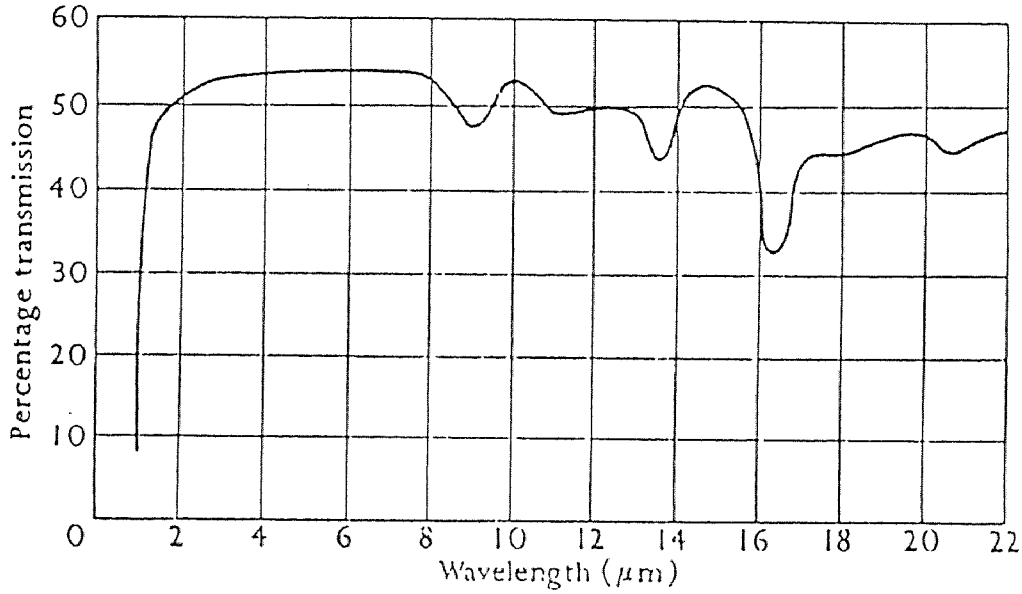

Figure 4.5 Transmission of silicon, resistivity 150 Ω-cm, thickness 0.05 cm.

A sample of silicon, 780A thick, was e-beam evaporated on sapphire. An FTIR spectroscopy was performed on the sample and the reflectance (Figure 4.6a) and transmittance (Figure 4.6b) were obtained. The refractive index (n) and extinction coefficient (k) were calculated from the transmission data obtained by FTIR. The values of n and k obtained were used in the filter design program. α is the absorption coefficient and f_1 and f_2 are the program iteration coefficients.

Table 4.1 Optical constants of silicon

$\lambda(\mu m)$	n	k	α	f_1	f_2
0.8	2.91	0.0	0.0	-2.38E-03	1.71E-07
0.9	3.13	0.0	0.0	-2.82E-03	1.59E-06
1.0	3.21	0.0	0.0	-2.28E-03	2.57E-06
1.1	3.24	0.0	0.0	-1.02E-03	3.90E-06
1.2	3.25	0.0	0.0	-7.29E-04	1.74E-07
1.3	3.25	0.0	0.0	-2.08E-03	2.03E-06
1.4	3.26	0.0	0.0	-2.86E-03	-1.86E-06
1.5	3.26	0.0	0.0	-1.87E03	1.62E-06
1.6	3.26	0.0	0.0	-4.35E04	-1.11E-07
1.7	3.26	0.0	0.0	-2.00E-03	-4.70E-07
1.8	3.27	0.0	0.0	-3.87E-04	-1.07E-06
1.9	3.27	0.0	0.0	-7.36E-04	-9.64E-07
2.0	3.26	0.0	0.0	-3.10E-04	-6.15E-07

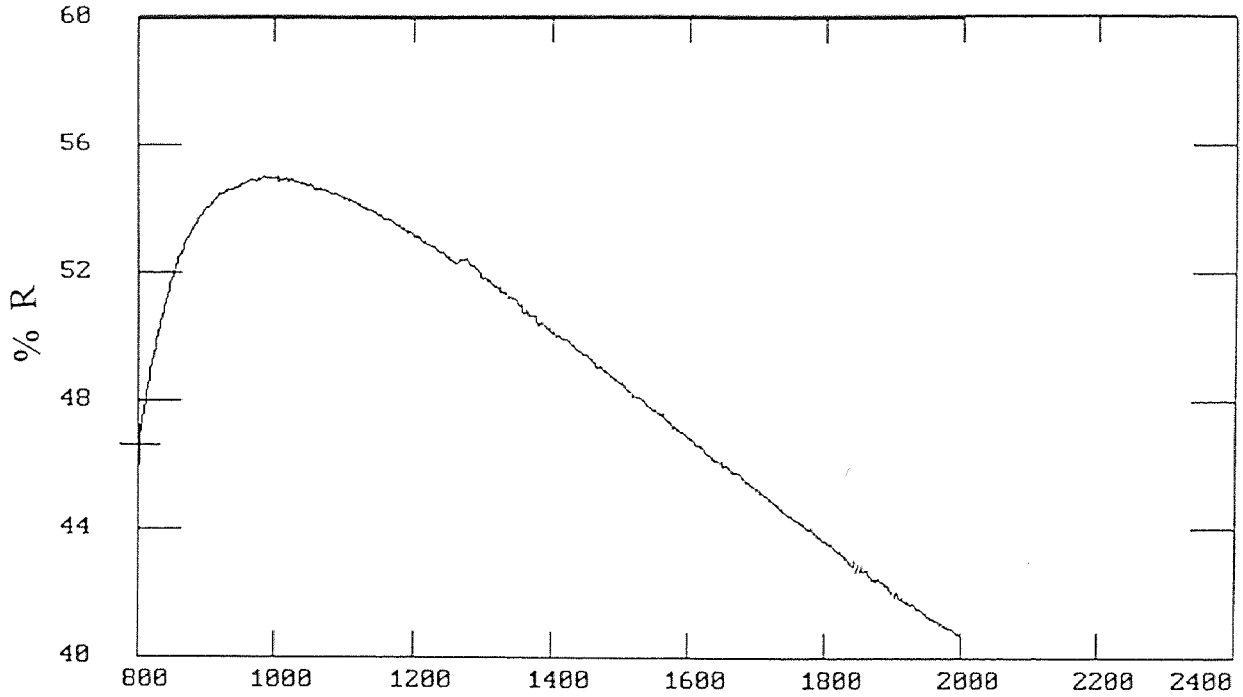

(a)

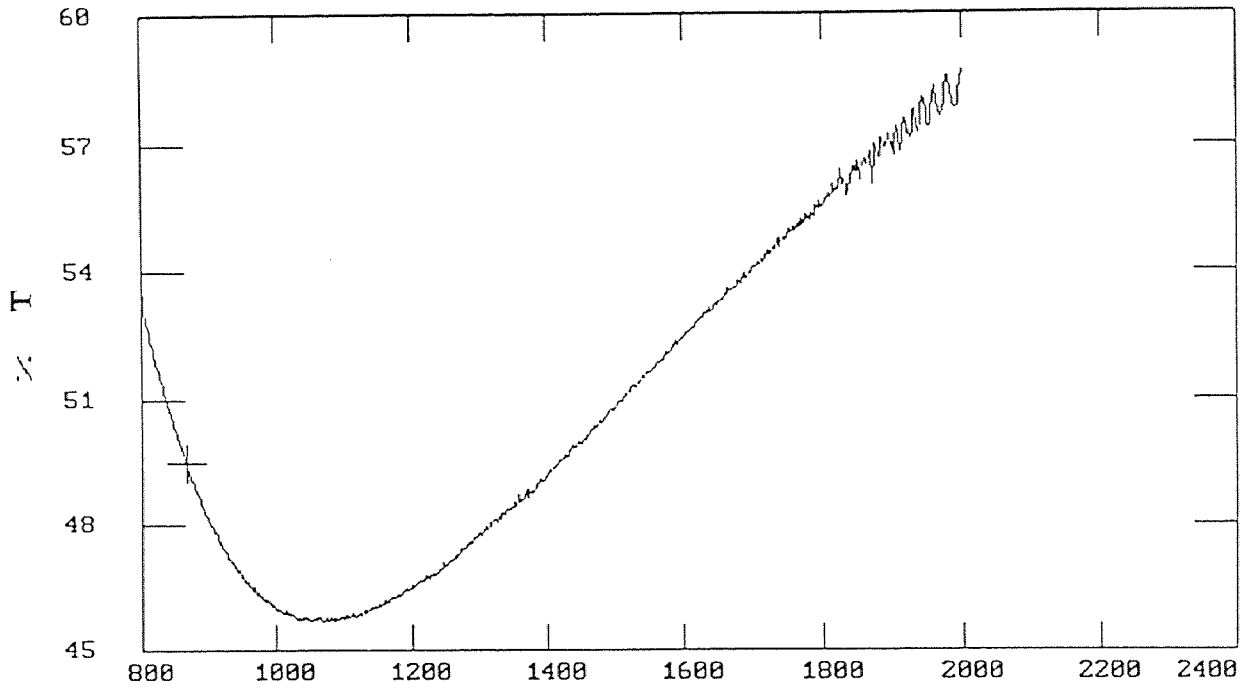

(b)

Figure 4.6 (a) Reflectance and (b) Transmittance of silicon in the range of 800 to 2,000 nm.

4.4 Silicon Dioxide (SiO_2)

The room-temperature optical properties of SiO_2 have been the subject of numerous studies. However, a few attempts have been made to analyze this information to obtain a self-consistent set of optical constants, n and k, for this material, especially in the regions of strong absorption in the infrared and vacuum ultraviolet[35]. The measured k values can be strongly affected by impurity and defect absorption. For SiO_2, the presence of water or (OH) absorption in the samples makes the determination of the intrinsic k values extremely difficult in certain domains of the infrared spectral region.

SiO_2 was e-beam evaporated onto a double-side polished silicon wafer. Two samples were prepared - one was on a halfpiece and was 3,000A thick, while the other was on a quarter piece, having a thickness of 2,700A. FTIR spectroscopy was performed on both the samples. From the transmission curves it can be seen that both the samples have similar optical characteristics (Figure 4.7).

During the deposition of SiO_2, if proper deposition conditions are not maintained, rise in the strong absorption bands occur in the infrared[38]. Infrared spectroscopy is a useful tool for investigating and evaluating SiO_2 films, as it is a non-destructive technique and the films can be examined both before and after subjecting them to various chemicals or ambients at elevated temperatures. SiO_2 is affected by moisture in the chamber and will show a dissolution of the film[39] which can be detected by weight loss and film-thickness decrease, or will show a significant amount of moisture in the film as seen by the presence of hydroxyl absorption in the 2.5 to 5 μm region of the spectrum (figure 4.8). Due to the hydroxyl absorption band, there is too much scatter in the region of the design wavelength. Hence, SiO_2 was not used as the low index material for the filters.

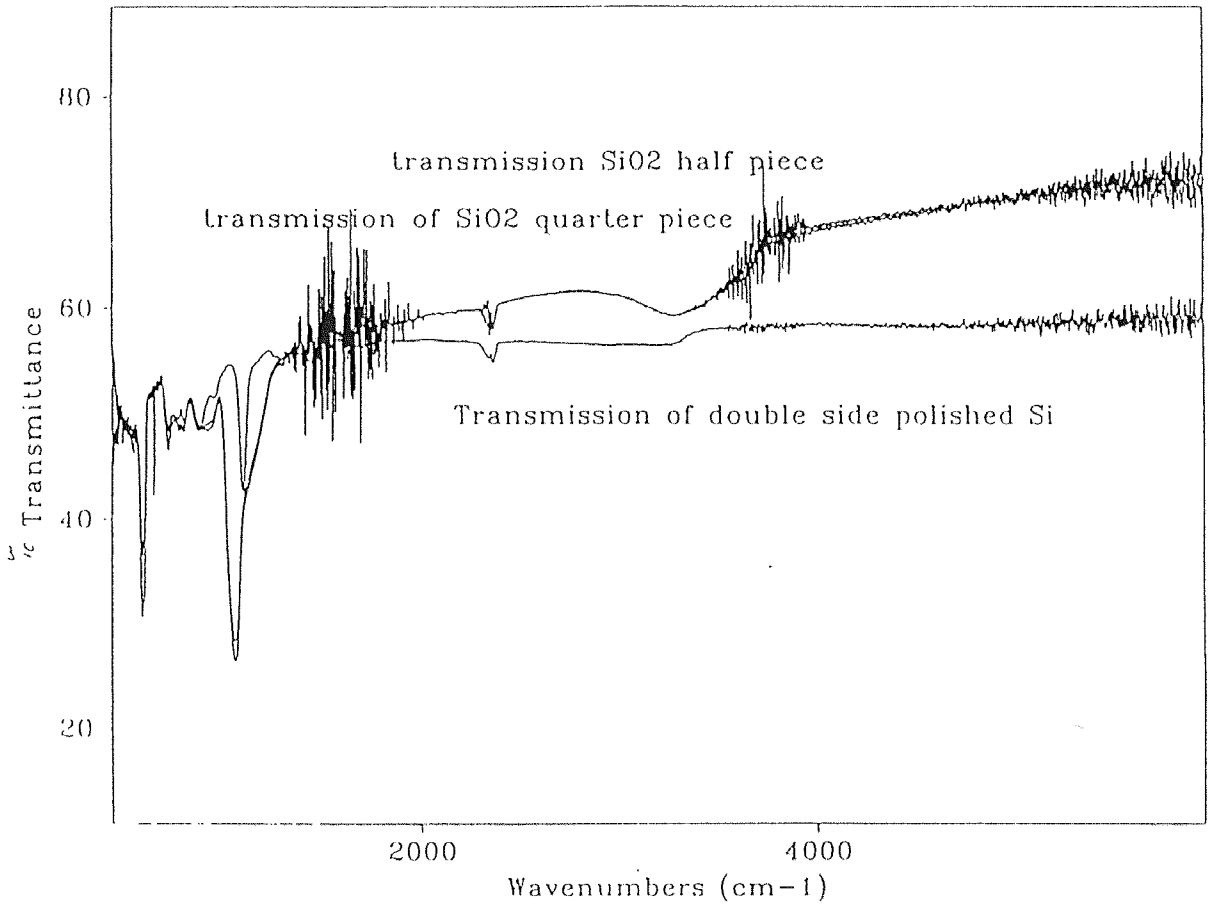

Figure 4.7 Transmission through the half piece sample (3,000A SiO_2 on Si) and the quarter piece (2,700A SiO_2 on Si) compared to double side polished Si wafer. Characterization performed at AFR.

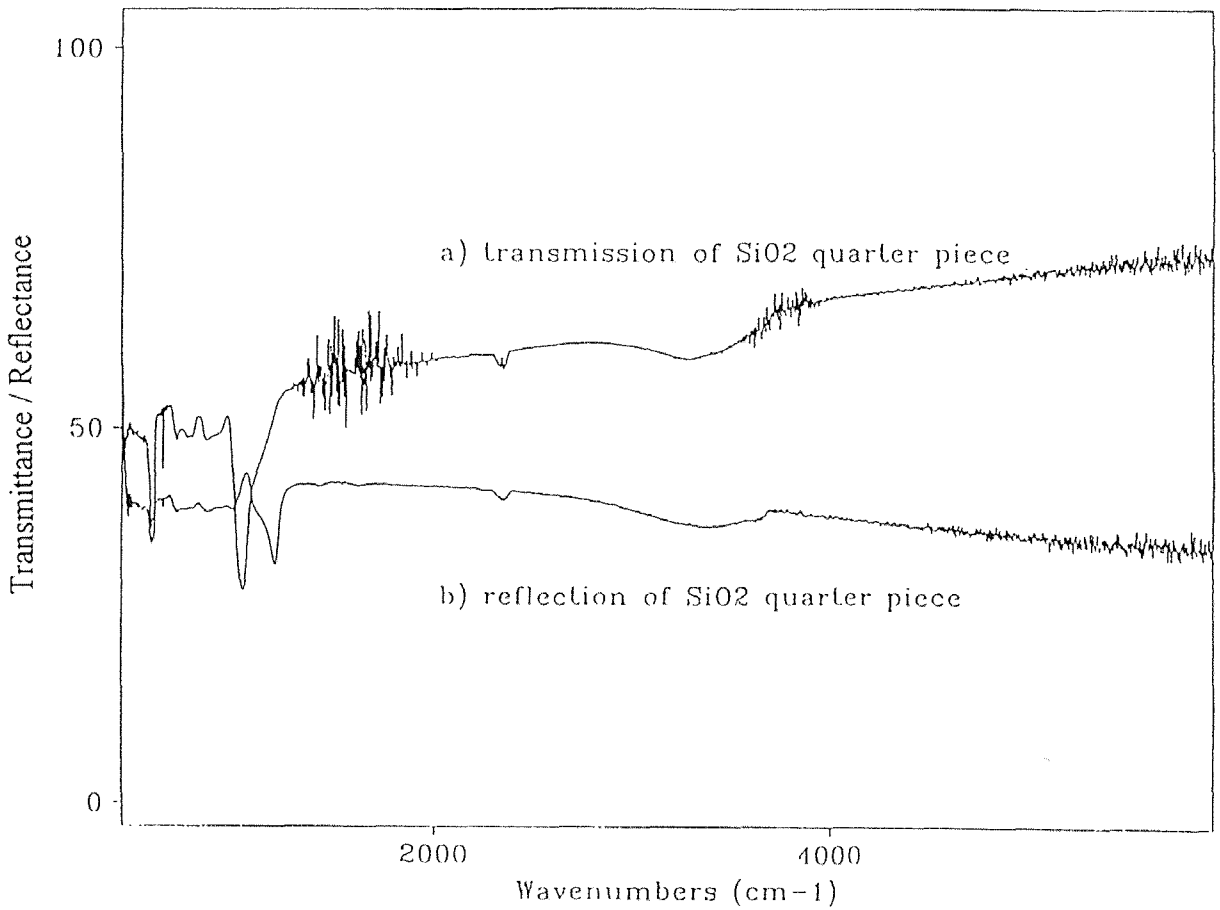

Figure 4.8 Transmission and reflection of 3,000A thick SiO_2 sample on double side polished Si. Characterization performed at AFR.

Optical constants (n and k) determined from reflectance measurement of both the samples were same and are given in Figure 4.9. Reflectance of the samples on the quarter piece and the half piece, overlayed with predictions using the optical constants, n and k, obtained in Figure 4.9 are shown in Figure 4.10. This projected curve shows a perfect fit for both the samples to the original reflectance curve.

From the optical charactestics curves of the two samples, it can be concluded that the optical components, required for the filter, remains similar over different thicknesses and that reproducibility of the layer characteristics can be achieved by careful control of the process conditions.

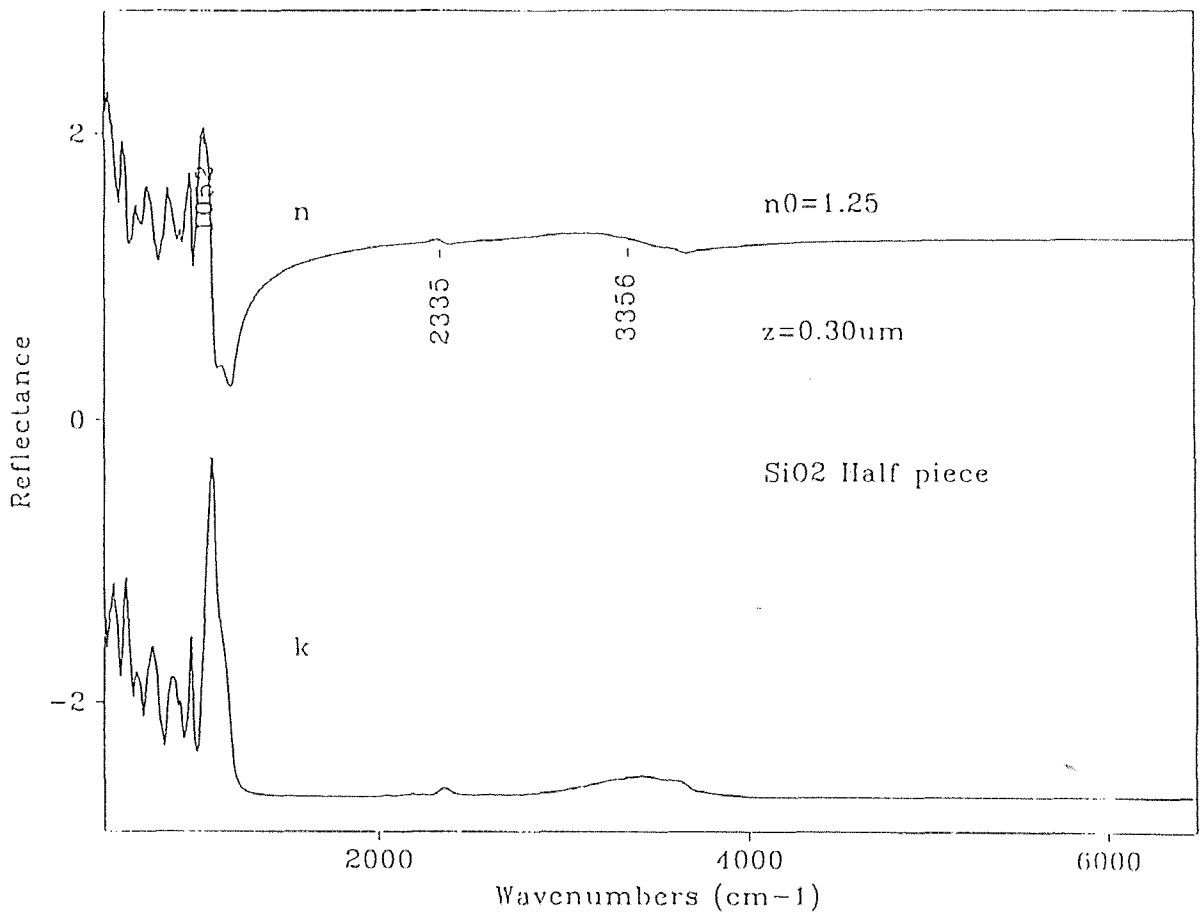

Figure 4.9 Optical constants (n and k) determined from reflectance measurement of 3,000A thick SiO_2 sample on double side polished Si. Characterization performed at AFR.

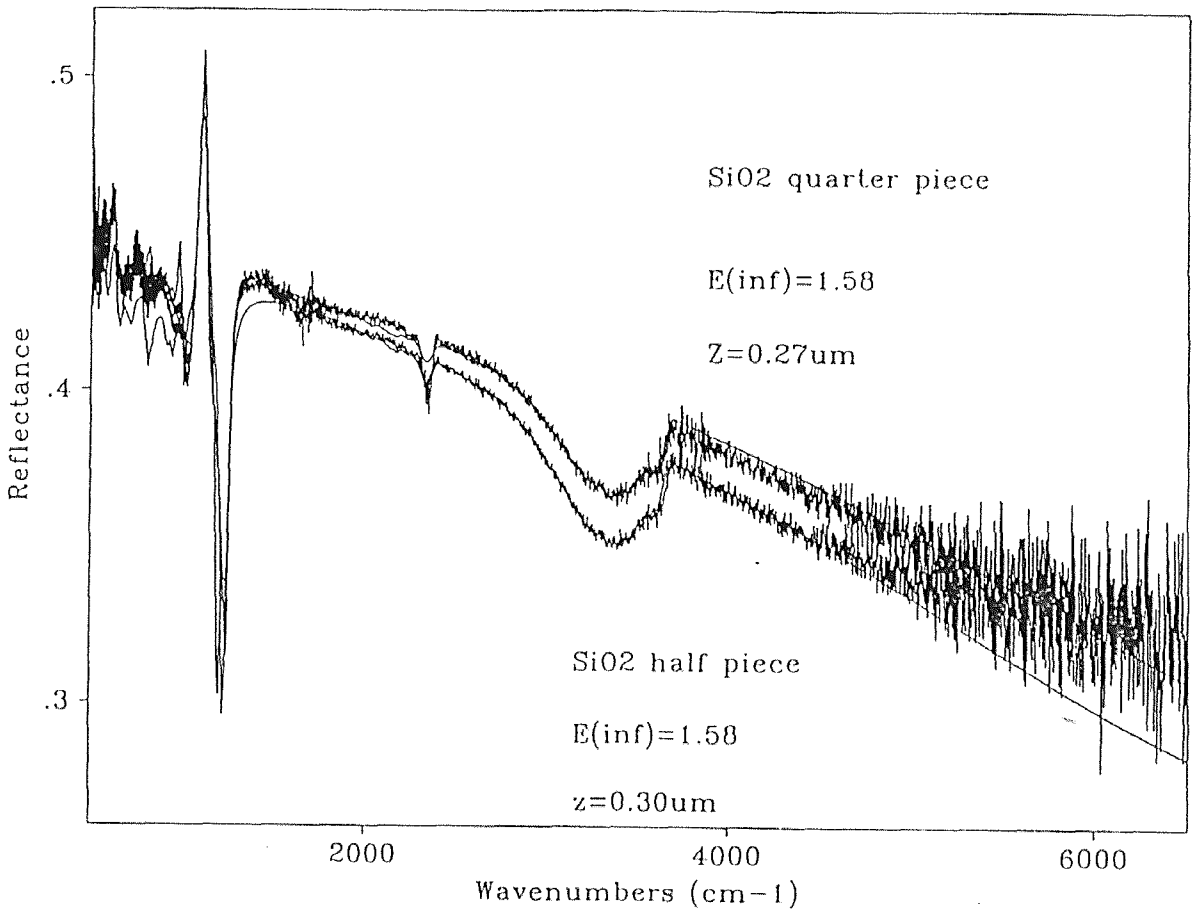

Figure 4.10 Reflectance of both the SiO_2 samples overlayed with predictions using n and k. Characterization performed at AFR.

4.5 Sapphire (Al_2O_3)

In recent years, artificial sapphire or Al_2O_3 has become available in a variety of shapes, in fairly large sizes. Al_2O_3 is highly transparent between 0.2 and 5.5 μm, and is mechanically strong, hard, and insoluble in water[40]. In addition, it is chemically inert, and will withstand high temperatures without changing its characteristics. This combination of properties makes Al_2O_3 a useful optical material, and it has found wide applications as window and dome material. The melting point is just over 2000°C, and the coefficient of expansion about 5.5×10^{-6}/°C. The thermal conductivity of Al_2O_3 is about 40×10^{-4} cal/s/cm/°C.

A 2000A thick sample of Al_2O_3 was prepared for FTIR spectroscopy by e-beam evaporation in an oxygen-enhanced environment. The reflectance and transmittance spectra were obtained (Figure 4.11). The refractive index (n) and extinction coefficient (k) were calculated from the transmission data obtained by FTIR. These values of n and k were used in the filter design software.

Table 4.2 Optical constants of Al_2O_3

λ(μm)	n	k	α	f_1	f_2
1.0	2.83	0.0	0.0	-5.83E-03	4.30E-08
1.1	1.91	0.0	0.0	3.76E-05	-1.23E-07
1.2	1.77	0.0	0.0	-2.36E-04	-5.37E-07
1.3	1.72	0.0	0.0	-4.79E-04	-2.64E-08
1.4	1.69	0.0	0.0	-7.90E-05	-1.12E-07
1.5	1.67	0.0	0.0	-2.13E-04	-2.94E-07
1.6	1.67	0.0	0.0	-7.01E-04	-1.37E-07
1.7	1.67	0.0	0.0	-1.32E-05	3.01E-09
1.8	1.68	0.0	0.0	-7.41E-04	-2.17E-08
1.9	1.69	0.0	0.0	-7.00E-04	1.12E-07
2.0	1.7	0.0	0.0	-4.41E-04	-1.46E-07

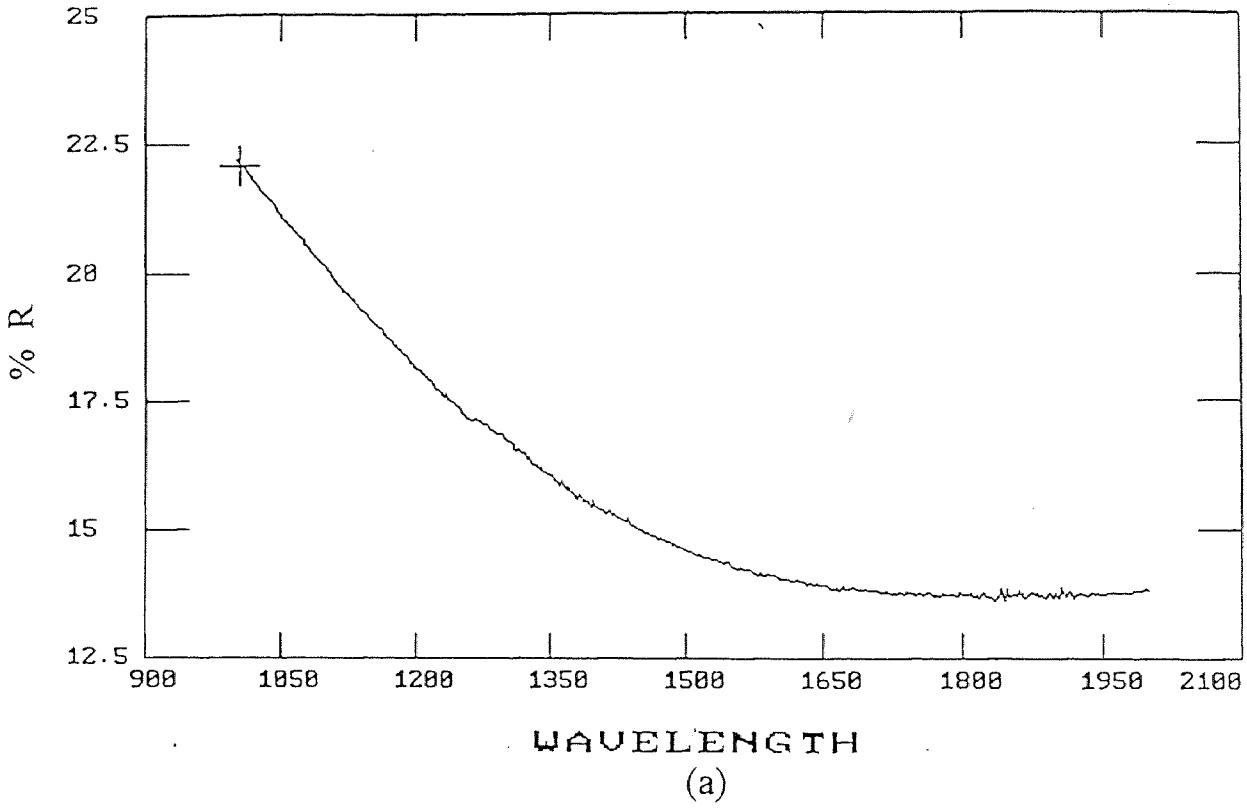

(a)

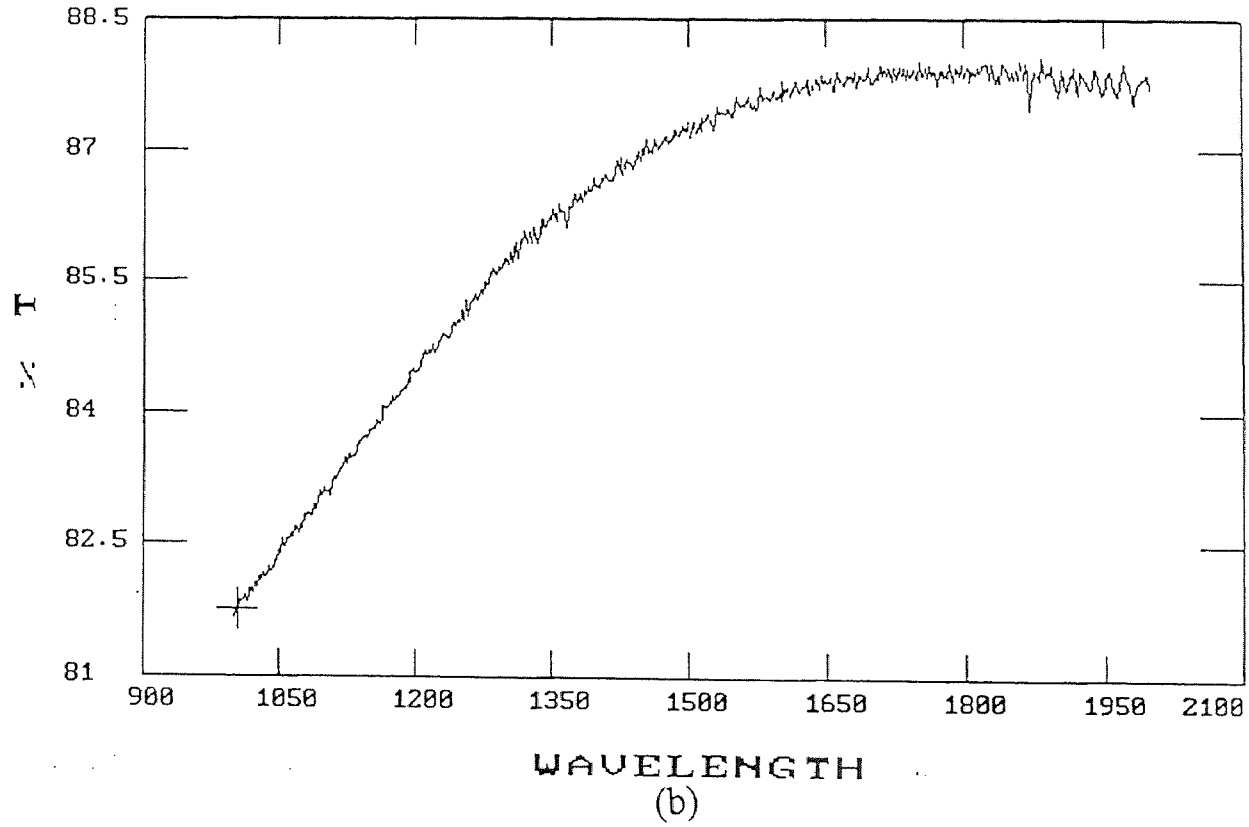

(b)

Figure 4.11 (a) Reflectance and (b) Transmittance spectrum of Al_2O_3 in the infrared region.

CHAPTER 5
FILTER PERFORMANCE

5.1 Introduction

The performance specification of a filter is a statement of the capabilities of the filter[40]. There is no systematic method for specifying the details of performance. Again, no absolute requirement for performance exists, only that the performance should be as high as possible within the permissible limits of complexity. The final specification is, thus, a compromise between what is desirable and what is achievable.

For a narrowband Fabry-Perot filter, the main parameters are peak wavelength, peak transmission, bandwidth, and rejection ratio. These parameters describe the filters fully and the performance of the filter depends on them.

5.2 Fabrication of Filters

The filters have been fabricated in an optical coater of a standard design (Figure 5.1). The stainless steel chamber has a front opening door for convenient access. The system is equipped with a cryo-pump and mechanical pump with gas purge. A glow discharge may be used for cleaning during the pump down period.

The chamber contains two electron beam guns with associated shutters and quartz crystal monitors for deposition rate control. A planetary substrate holder provides for uniformity of substrate coatings. An optical monitor measures transmission on a test piece mounted in the same plane as the substrates while a test piece changer allows seperate test pieces for different

parts of deposition. Substrate heaters can be used for deposition at higher temperatures.

Initially, filters had been designed using SiO_2 as the low index material and Si as the high index material. Early tests indicated that SiO_2 was unacceptable because of the appearance of hydroxyl absorption peaks in the spectral ralnge of interest. Therefore, Al_2O_3 was substituted as the low index material.

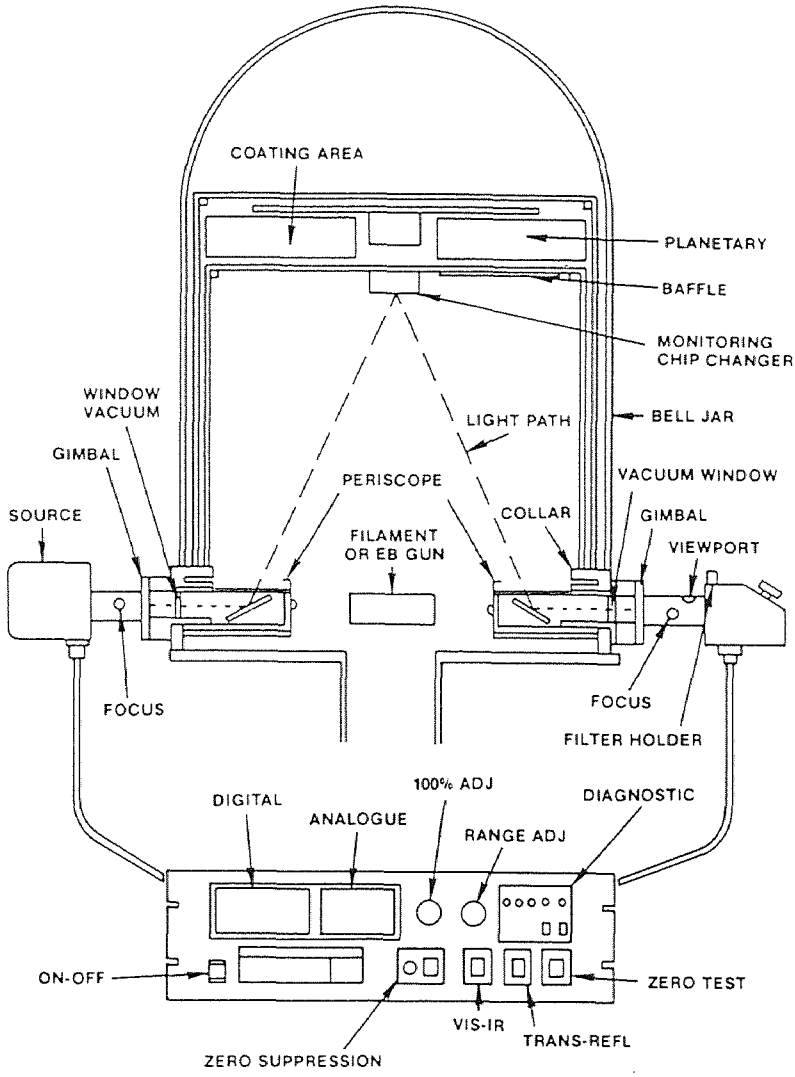

Figure 5.1 Evaporator configuration used in filter production.

The filters consists of 11 layers with a single aluminum layer at the center of the filter stack. A glass piece, with refractive index of 1.51, has been used as the test piece for optical monitoring. Since the first layer to be deposited on glass is Al_2O_3, the difference between the indices is very small. As such, the signal from the optical monitor is also very low. In order to get a larger signal, a quarterwave layer of Si is initially deposited. This does not affect the design of the filter since the substrate is also Si. A 1.33 μm filter has been used to monitor the thickness for the filter with peak transmission at 1.33 μm, while the monochromator has been set at 1.5 μm for the filter with center wavelength at 1.5 μm.

5.3 Results and discussion

The performance of the filters fabricated using the FILM*CALC 3.0 design specifications can be obtained from the transmission curves of the respective filters. Figures 5.2 and 5.3(a) and (b) correspond to Runs 1, 2 and 3 for the filters with peak transmission at 1.5 and 1.33 μm respectively. The performance of the filters are summarized in the following table:

Table 5.1 Performance of the fabricated filters

Filter Parameter	Run 1	Run 2	Run 3
Center Wavelength	1.5 μm	1.33 μm	1.42 μm
Peak Transmission	3%	10%	33%
Bandwidth	75 nm	75 nm	55 nm
Rejection	poor	poor	excellent

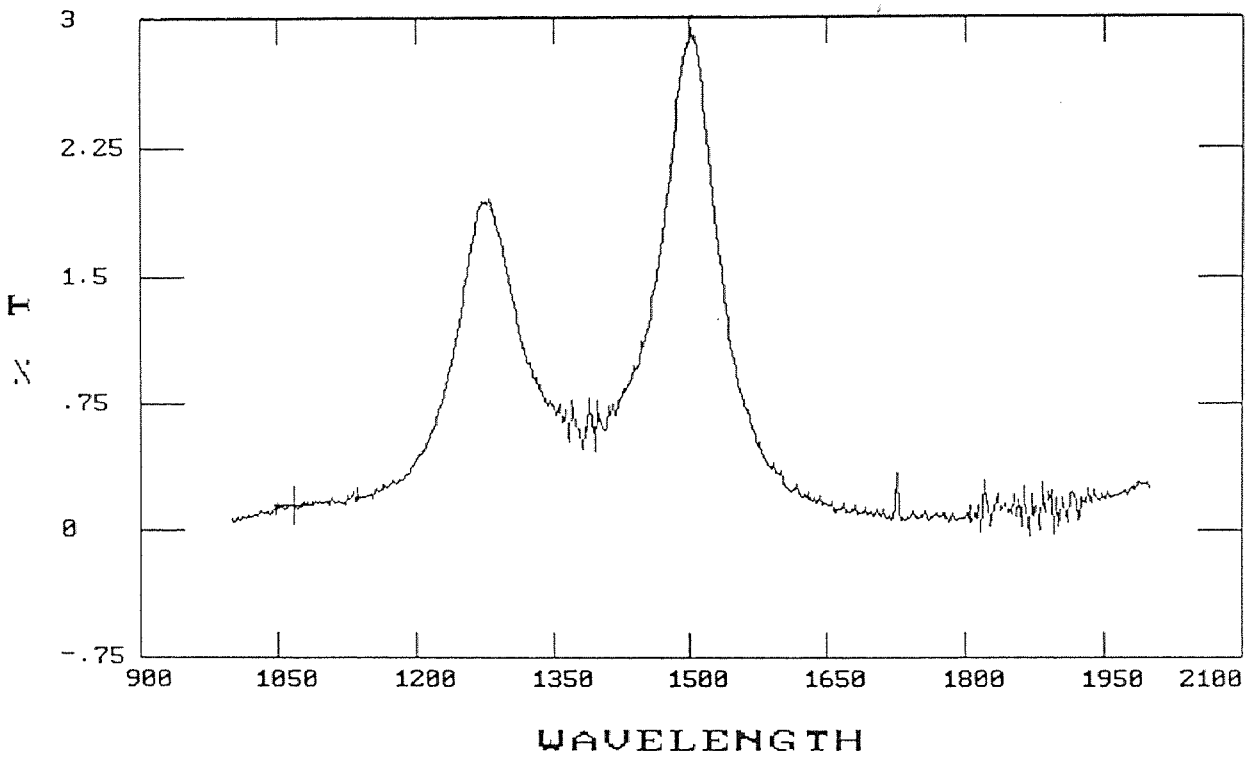

Figure 5.2 Actual transmission curve for the filter with peak transmission at 1.5 μm. The curve indicates poor rejection and transmission and two peaks for Run 1. The wavelength has the unit of nm.

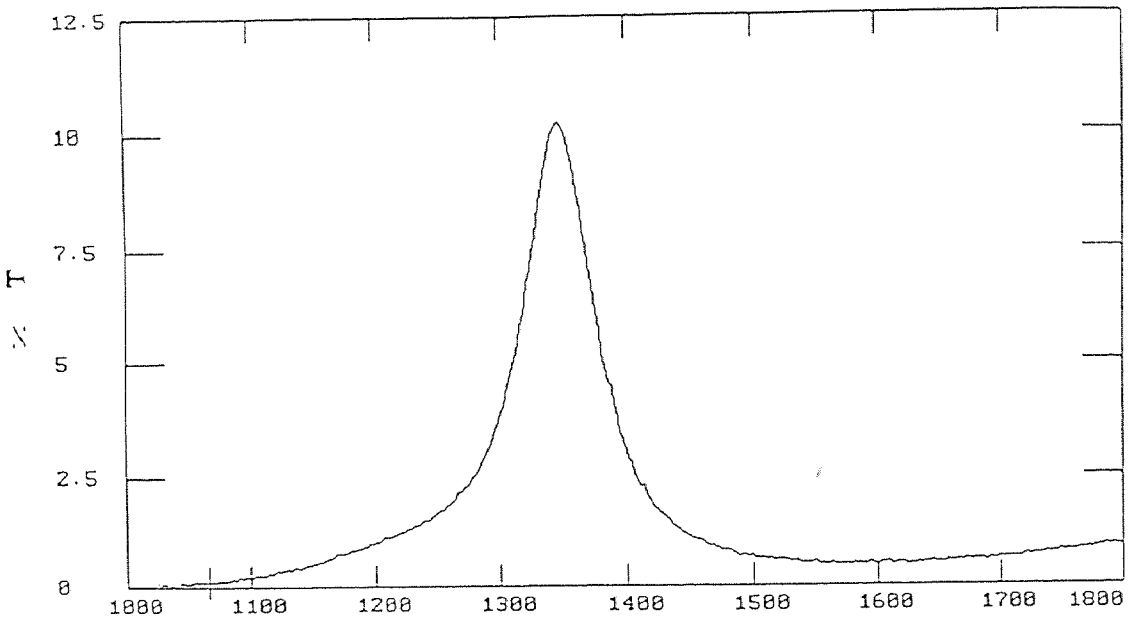

(a)

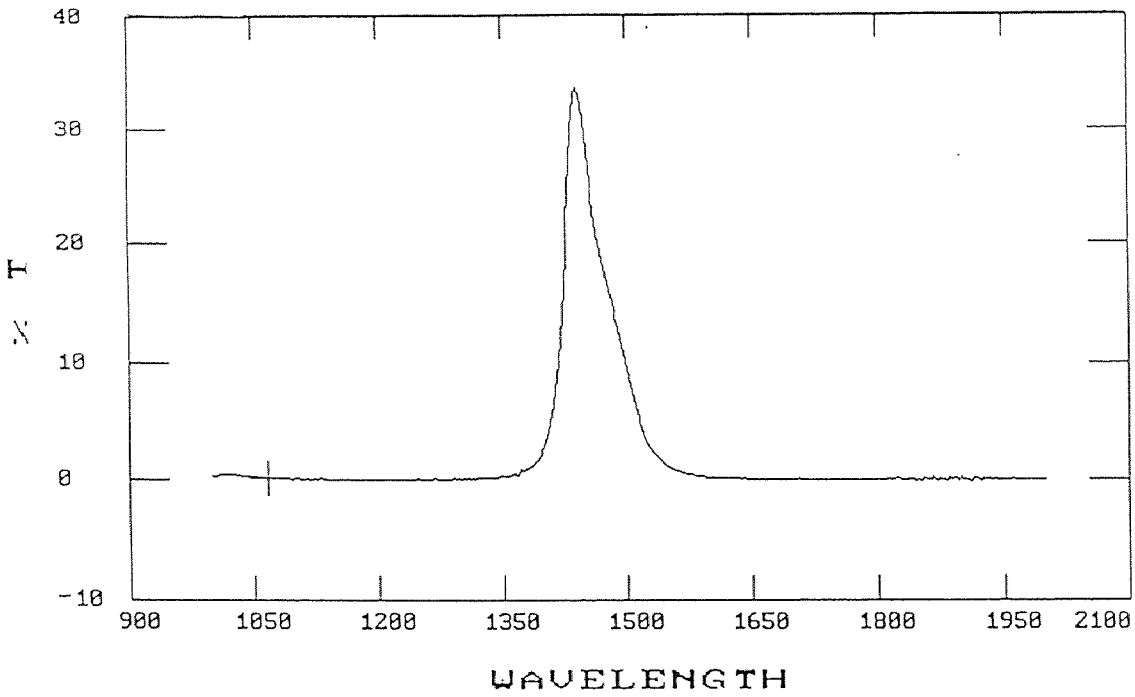

(b)

Figure 5.3 Actual transmission curves for the filter with peak transmission at 1.33 μm. (a) Run 2 - The curve shows poor transmission and rejection. (b) Run 3 - The curve indicates excellent transmission, but a shift in the peak transmission wavelength. Wavelength has the unit of nm.

The filters obtained from Runs 1 and 2 show poor transmission and rejection, while the filter obtained from Run 3 indicates a much higher transmission and excellent rejection, yet the center wavelength has been shifted to 1.42 μm. All these factors can be attributed to the thickness discrepancy of the layers with that of the design specifications. The optical thicknesses of the layers monitored for quarter wavelength and the physical thicknesses for Runs 1, 2, and 3, obtained by the quartz crystal microbalance is summarized in Table 2:

Table 5.2 Layer thicknesses for the fabrication of filters

Depositing Layer	Layer #	Layer Thickness	Run 1 1.5 μm	Run 2 1.33 μm	Run 3 1.33 μm
Si		1/4λ	964	1017	1592
Al_2O_3	1	1/4λ	2410	2688	2915
Si	2	1/4λ	1031	1070	1293
Al_2O_3	3	1/4λ	2358	2576	3533
Si	4	1/4λ	945	1098	1514
Al_2O_3	5	1/2λ	4900	5497	6395
Al	6		200	300	300
Al_2O_3	7	1/2λ	4750	5132	5927
Si	8	1/4λ	1027	945	1516
Al_2O_3	9	1/4λ	2413	2500	3829
Si	10	1/4λ	1370	1300	1356
Al_2O_3	11	1/8λ	1204	1100	1500

The physical thicknesses for silicon and Al_2O_3 layers for the filter with center wavelength at 1.5 μm is 1077 and 2351A respectively. For the filter with peak transmission at 1.33 μm, the physical layer thicknesses of silicon and Al_2O_3 are 955 and 2085A respectively. From Table 5.2, it can be seen that the deposited layer thicknesses are almost close to the desired values. This variation in thickness monitoring can be attributed to a few reasons. Run 1 was monitored through the optical monitor and using a monochromator to select the wavelength. Since there is a loss in intensity in every stage of the system, the monitoring signal was low and as such detecting the turning point was very difficult. Run 2 shows an improvement since a narrow band filter with a peak transmission at the monitoring frequency of 1.33 μm was used instead of the monochromator. This reduces the loss in the system and also more signal is transmitted through the filter. Yet, the signal was not sufficient enough for good monitoring due to the loss of light intensity in the fiber optics.

The transmission curve for Run 1 shows double peaks. This was due to the decrease in the metal layer. The design specification suggests the deposition of 300A of Al, whereas only 200A was deposited.

There is a drastic change in the performance of the filter for Run 3. The transmission curve shows an increase in the peak transmission to nearly the desired design value. A different approach was taken for the optical monitoring of this filter. Light was directly shone on the test piece and the reflected light was passed through the monitoring filter, thus avoiding the monochromator and fiber optics. The monitoring signal was sufficient enough for controlling the thickness.

The optical monitor is not cotrolled by any procees controller. Thus the monitoring totally depended on the judgement of the operator. Hence,

human errors should also be taken into account for the difference in the layer thicknesses. This error can be reduced by using a microprocessor-controlled optical monitor or by repeating the fabrication process over and over till the operator has perfected the monitoring techniques.

CHAPTER 6
SUMMARY AND FUTURE WORKS

6.1 Summary

The narrow bandpass filters were initially designed using the FILM*CALC 3.0 software with Si, SiO_2 and Al as the materials of choice. As such, the deposition conditions were set up for each of these materials so that reproducibility can be achieved. FTIR spectroscopic studies were performed on Si and SiO_2 to obtain the optical properties of the materials. From these studies, hydroxyl absorption band was detected in SiO_2 within the spectral region of the design specifications. Therefore, SiO_2 was substituted by Al_2O_3 as the low index material and designs were made accordingly. The design parameters and the number of layers did not change, because the refractive index of Al_2O_3 and SiO_2 are very close to each other at a given wavelength.

The values of refractive index (n) and extinction coefficient (k) obtained from the spectroscopic studies of the materials were now used as actual data and the filters were again designed to meet the required filter specifications.

The filters have been fabricated in an optical coater with the thickness controlled by an optical monitor. Initial runs indicate a low performance of the filters fabricated. This can be attributed to the optical monitor itself. Energy of light in the infrared is low, and there is a loss of energy in every stage, i.e. monochromator and fiber optics, of the monitor. This gives a small detector signal, making detection of the termination point of each layer extremely difficult.

During Run 3, the monochromator and the fiber optics has been eliminated from the path of the monitoring signal. Light is projected directly

on the test piece and the reflected light is collected by the detector. As the losses are minimized, there is a big improvement in the monitoring signal. With the enhancement of detection signal for the termination point, the filter shows a greater improvement in performance.

6.3 Future Works

The present work suggests that filters with peak transmissions and narrow passbands, as required by the design specification for the multi-wavelength IR camera, can be achieved. The fabricated filter showed excellent transmission and narrow band-pass with peak transmission at 1.33 μm. These filter parameters can be improved with careful monitoring and control of the fabrication process. Two more filters with peak transmission at 2.66 and 4.0 μm will be fabricated and their performance evaluated. A set of striped filters, comprising of these three individual filters will be fabricated on a 4" silicon wafer.

Presently, work is in progress to determine the optimum process conditions for patterning of the filter. The process is complicated because of the difficulty in etching Al_2O_3 films.

At the end of the project, we anticipate that a set of striped filters with desired spectral characteristics will be available for deployment with IR camera, thus providing it with the definition of the wavelengths for multi-wavelength imaging.

APPENDICES

APPENDIX I

FILTER DESIGN PROGRAMS

The filters were designed using the FILM*CALC 3.0 software by FTG Associates. The following are the design programs for the filters with peak transmissions at 1.33 and 1.5 μm respectively.

FILM*CALC DESIGN FTG Software, Princeton, NJ

Si, Al_2O_3, Al at 1.5 μm on Si						
Design Wave 1.5 μm						Angle 0°
Design (from substrate) - File NJIT-1.5						
1 .25L	2 .25H	3 .25L	4 .25H	5 .4855L	6 .03M	
7 .4855L	8 .25H	9 .25L	10 .25H	11 .125L		
Film Indices - file NIT-1.5				L,H: QWOT= .25	M: μm	
Indx Symb	File or $Function	A (n)	B (k)	C	D	E
AIR		1	0	0	0	0
SUB	Si	0	0	0	0	0
L	Al_2O_3	0	0	0	0	0
H	Si	0	0	0	0	0
M*	Al	0	0	0	0	0

'*' Physical Thickness

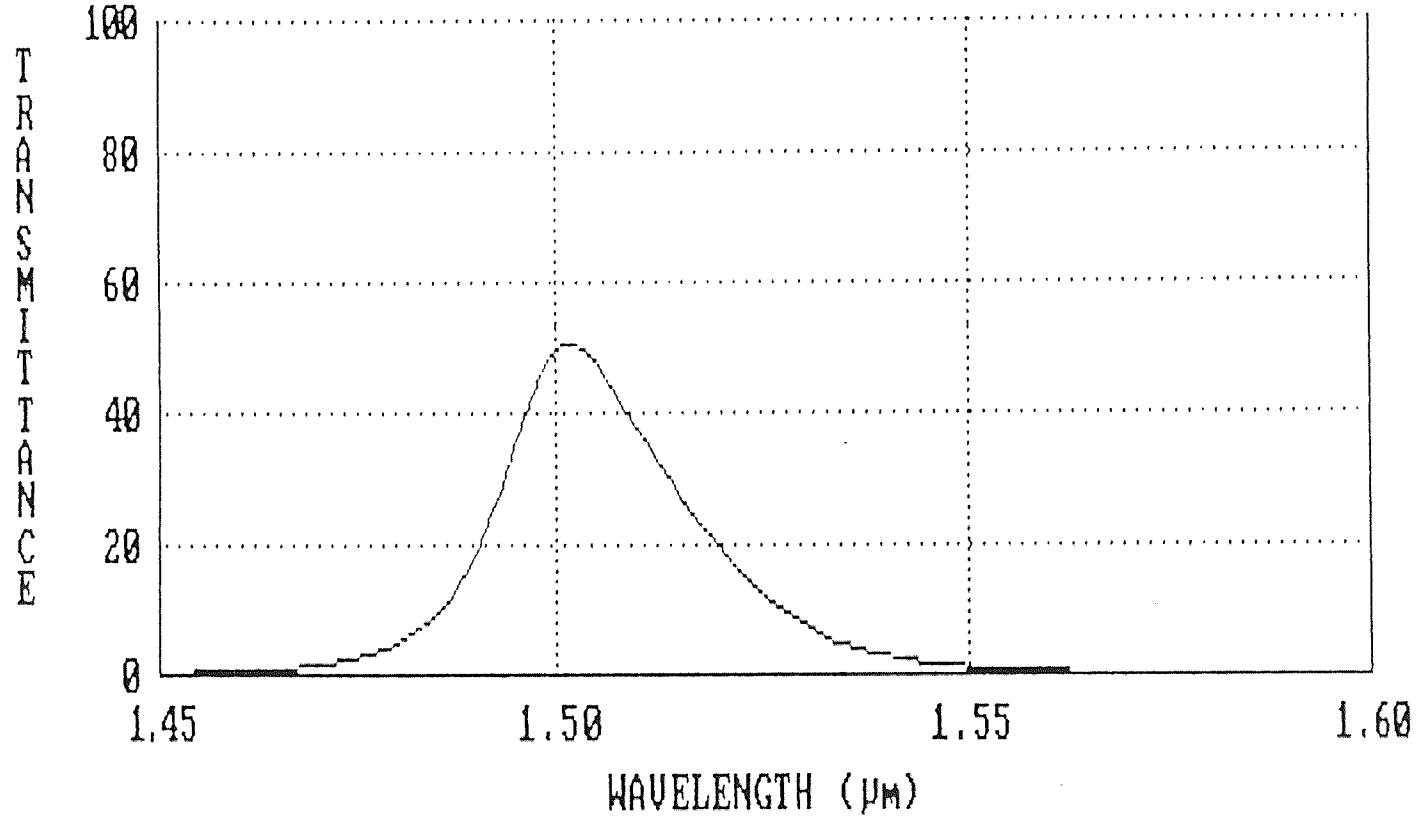

Figure 1 Transmission curve for the filter with peak transmission at 1.5 μm.

FILM*CALC DESIGN FTG Software, Princeton, NJ

Si, Al_2O_3, Al at 1.33 μm on Si						
Design Wave 1.33 μm						Angle 0°
Design (from substrate) - File NJIT-1.33						
1 .25L	2 .25H	3 .25L	4 .25H	5 .488L	6 .03M	
7 .488L	8 .25H	9 .25L	10 .25H	11 .125L		
Film Indices - file NIT-1.33				L,H: QWOT= .25	M: μm	
Indx Symb	File or $Function	A (n)	B (k)	C	D	E
AIR		1	0	0	0	0
SUB	Si	0	0	0	0	0
L	Al_2O_3	0	0	0	0	0
H	Si	0	0	0	0	0
M*	Al	0	0	0	0	0

APPENDIX II

DENTON VACUUM MODEL 32 C BOX COATER

Vacuum chamber description

The vacuum chamber is an all stainless steel chamber measuring 26" wide, 30" deep, and 32" high. The chamber is split on a vertical axis with a door on the front of the system. The deposition chamber has an o-ring seal at the bottom of the bell jar to mate the chamber with the baseplate. This allows the chamber to be removed from the pumping system for modifications, maintenance, or other purposes. Access for normal operation is through the front door, which contains three 4" view ports with manual shutters.

The chamber is water-cooled, using stainless steel U channel. The U channel provides a neat appearance, is easy to keep clean, and provides a high area of direct water-cooling of the chamber surface. Internal support for aluminum foil is provided to allow easy cleaning of the chamber.

The system is leak-tight when pumped to the low 10^{-6} Torr range. System ultimate vacuum is in the low 10^{-7} Torr range. The chamber and the door is electro-polished.

Substrate fixture/planetary system

DVI's standard high temperature tilt action, friction drive planetary with 3 12" planets is included. This planetary system is specified to work continuously at 400°C substrate temperature. It includes one main support bearing rated for over 10,000 lbs. continuous weight-carrying capacity. The bearing is mounted on a directly water-cooled hub which is cooled by a full annular ring water cavity rather than tubing. The central support hub has an internal diameter of approximately 9" to allow the location of an optical monitor chip

changer, quartz crystal monitor sensor, and thermocouple in the center of the chamber. The planetary top plate has a window (to be used for transmission monitoring), a Conflat flange for a quartz crystal monitor, a thermocouple feedthrough, and provision for actuation of a glass changer.

The planetary system is protected from jamming by torque limiters, which include speed ramps (both start and stop). Rotation speed is adjustable from the front panel of the unit.

Model STIH-270-1 Four-hearth Electron beam source

The Airco Temescal Model STIH-270-1 Electron Beam Gun has four crucibles that are evenly spaced and are presented sequentially to the electron beam. While the contents of one crucible is being evaporated, the other three are concealed to protect them from stray beams and debris. The design prevents cross-contamination of evaporants between the crucibles. A gear ring on the base of the crucible assembly mates with the drive gear assembly. Both the crucible brazement assembly and the baseplate are water-cooled. Watre is fed into the baseplate through the crossover at the knurled connector and drains at the top of the crucible assembly.

The magnetic fields that direct and focus the electron beam are supplied by a hermetically sealed deflection electromagnet, a main-field permanant magnet, two pole pieces, and two pole-piece extensions. The deflection coil is used to accomplish X-Y beam sweeping. Its wide frequency range makes it a versatile evaporation tool. The field of the permanent magnet, located inside the back of the system, is used to confine the beam to the hearth area.

APPENDIX III
IC 6000 DEPOSITION CONTROLLER

General Description

The IC 6000 is based on a resonating quartz crystal sensor, which provides both accurate film measurement and total deposition control. The IC 6000 incorporates unsurpassed programming capability, with 6 complete and independent film programs each of which contain 37 programmable parameters. For automatic sequencing of multilayer processes, the unit may be programmed to automatically control a process of upto 32 layers, with each layer controlled by any one of the six film programs. For systems with multi-process requirements, the IC 6000 will store three separate process sequences, so that changing from one process to another is as simple as programming a desired process to run. External connections can link the three processes into a single process of upto 96 layers.

Several unique functions are included in this list of 37 film program parameters. Two rate ramps, for example, provide complete control of rate changes during each film deposition. Tighter rate control may be established on even the slowest responding sources, by programming the control parameters - gain, approach, and limiter. The "presoak enable" feature reduces cycle time by allowing a second source to presoak, while the unit is simultaneously controlling the first layer source.

Three new front panel functions have been provided for ease of operator control. A process sequence that has been interrupted may be continued from the interrupted layer or can be reset to its beginning layer with the push of a button. In addition, a film program can be reset to its beginning without losing previous sequence information, or aborting an entire process.

The IC 6000 Data display provides the user with process control information. This single display gives rate, thickness, power, process time, and crystal condition information, plus an analog record of the quality of rate control. A message on the Data display describes system malfunctions, process status, and abort conditions when a process or film terminates.

Film Sequencing

A film sequence begins with a start command and ends when the film in process reaches the idle phase. Any process control between these events is determined by the values programmed in the 37 possible film parameters. A film sequence consists of sixteen possible phases, with a phase being defined as one process event. These phases are described below:

	Phase	Condition
1.	Ready	Shutter closed; will accept a start command
2	Rise 1	Shutter closed; source rising to Soak 1 power
3	Soak 1	Shutter closed; source maintained Soak 1 power
4	Rise 2	Shutter closed; source rising to Soak 2 power
5	Soak 2	Shutter closed; source maintained Soak 2 power
6	Shutter delay	Shutter closed; rate control
7	Deposit	Shutter open; rate control
8	Rate Ramp 1	Shutter open; rate control;desired rate changing

9	Rate Ramp 2	Shutter open; rate control; desired rate changing
10	Feed Ramp	Shutter closed;source maintained at feed soak power
11	Feed Soak	Shutter closed; source maintained at feed soak power
12	Idle Ramp	Shutter closed; source changing to idle power
13	Idle Zero	Shutter closed; source maintained at zero power; will accept a start command
14	Idle Non-Zero	Shutter closed;source resting at idle power; will accept a start command
15	Manual	Shutter open; source power controlled by hand controller
16	Time-power	Shutter open; crystal failed;source maintained at average control power prior to crystal failure

It is not required to execute all IC 6000 film phases when a film is generated. For example, phases will automatically be skipped if the film parameters used to define that phase have been deleted. Or, in the case of parameters that cannot be deleted, phases will be skipped if the value is programmed to zero. (However, the idle phase of a film program will always be executed.) Finally deleting certain parameters will also cause others to be deleted. For example, when the programmed power level for phases Rise 1, Rise 2, and Feed Ramp is Zero, the corresponding soak phase will be automatically deleted and skipped in the film program. When the desired

control rate is programmed to zero, the entire deposit phase will be skipped. If no parameters have been programmed, the film will sequence immediately to the idle phase when a start command is executed.

When a film program finishes in an idle phase at a power level other than zero, a subsequent start command to this film will initiate the film program at the Rise2 phase, skipping both the Rise 1 and Soak 1 phases if they were programmed. If a Rise 2 phase is not present in the film program, the unit will sequence to the next viable phase-shutter delay, deposit feed ramp, idle ramp, or idle (in that order).

Manual power phase can be entered whenever the IC 6000 is not aborted or stopped. The shutter will always open and the final thickness event will be ignored. When the manual control phase is ended, the unit will sequence to the deposit phase, provided a rate other than zero has been programmed and the final thickness limit has not been exceeded. Any thickness accumulated while the unit was in manual mode will be retained when the manual phase is ended, and any next layer presoak operations will be terminated when the manual control phase is entered.

The recipe for the deposition control of each material is given in a tabular form. These process parameters are maintained during the filter fabrication for repeatability.

Recipe for Deposition Control of Materials

MATERIAL	Si	SiO_2	Al_2O_3	Al
GUN #	2	1	1	1
CRUCIBLE#	3	4	4	2
FILM #	5	5	1	2
PR.- START	3.9×10^{-6}	3.9×10^{-6}	3.9×10^{-6}	3.9×10^{-6}
PR- EVAP.			2.1×10^{-5}	
DENSITY	2.32	2.65	3.97	2.7
Z RATIO	0.712	1.00	0.336	1.08
TOOLING	75	86	81	65
SENSOR	1	1	1	1
SOURCE	1	1	1	1
GAIN	2	2	5	5
APPROACH	7	7	10	25
LIMITER	10	10	10	5
SOAK P1	22	18	18	18
RAMP T1	1:00	1:00	1:00	1:00
SOAK T1	1:30	:15	0:30	0:30
SOAK P2	24	20	22	23
RAMP T2	0:30	:30	0:30	0:30
SOAK T2	1:00	0:15	0:30	0:30
SHUT. DEL	0:30	0:30	0:30	0:30
RATE	4A/s	8A/s	10A/s	5A/S
FINAL THK	3000A	2500A	7000A	300A
THK LIMIT	3000A	2500A	7000A	300A
MAX PWR	36	23	37	34

APPENDIX IV
DENTON VACUUM OPTICAL MONITOR

System Description

The Denton Vacuum SD-10 Optical Monitor synchronously demodulates a chopped light source to make linear photometric measurements of reflectance or transmission of thin film optical coating as they are being deposited. This is accomplished by the generation of reference signal within the light source which is then passed to lock-in or demodulation circuitry at the heart of the SD-10 signal processing action. The use of this synchronous demodulation system allows the SD-10 to be used in full room light and in environments with fluctuating light levels and high ambient noise levels. Consequently, small signals buried in noise can be extracted without any loss in sensitivity, linearity, or with the introduction of instability of any kind.

The SD-10 Optical Monitor System includes a chopped light source (either conventional or fiber optics), with an internal reference photodiode and optics, and a receiver/detector (with narrow band-pass optical interference filter or monochromator) with pre-amplifier and optics to maximize low level signal detection and minimize cable pickup and noise.

The photocells convert light energy into electrical energy which is then passed to the detection/demodulation circuitry. The lock-in board compares the frequency of the reference signal to that of the raw input signal and extracts a dc voltage directly proportional to the reflected or transmited signal mixed with noise and ambient light fluctuations. This approach provides a high degree of noise immunity against background noise levels because only signals at the reference frequency are processed. With a narrow band pass filter or monochromator before the detector, the photocell sees esentially

monochromatic light which it converts to an electrical signal and passes to the optical monitor. As the coating is applied to a test piece in the optical pathway, the reflectance/transmission changes which occur are displayed by the optical monitor and output to a strip chart recorder. The receiver can be used to measure changes in either reflectance or transmission depending on the location of the detector within the unit. Two detectors may be mounted in one unit, with the option of selecting either reflectance or transmittance mode of monitoring from the front panel. The entire signal processing action of the SD-10 is packaged in a standard 19" rack mountable enclosure, and the light sources and detector units are flange or feed-through mountable, compatible with standard bell jar and box coater systems.

The optical monitoring curves for the filters with peak transmissions at 3.0 μm and 4.5 μm are given in Figures 1 and 2 respectively.

System set-up

A monitor system may be set up using conventional reflective optics or fiber optics either in conjunction with the conventioanl optics or independently. Variations are shown in Figures 1 through 4. For the 4.5 μm filter, two seperate test pieces are needed.

Basic System

A basic system includes the SD-10 Monitor instrument (1) with a modulated quartz halogen light source (2), a receiver/detector with filter holder (3) for reflective or transmission monitoring and connecting cables(Figure 3a). The detector is also available with a monochromator and with manual or computer compatible operation.

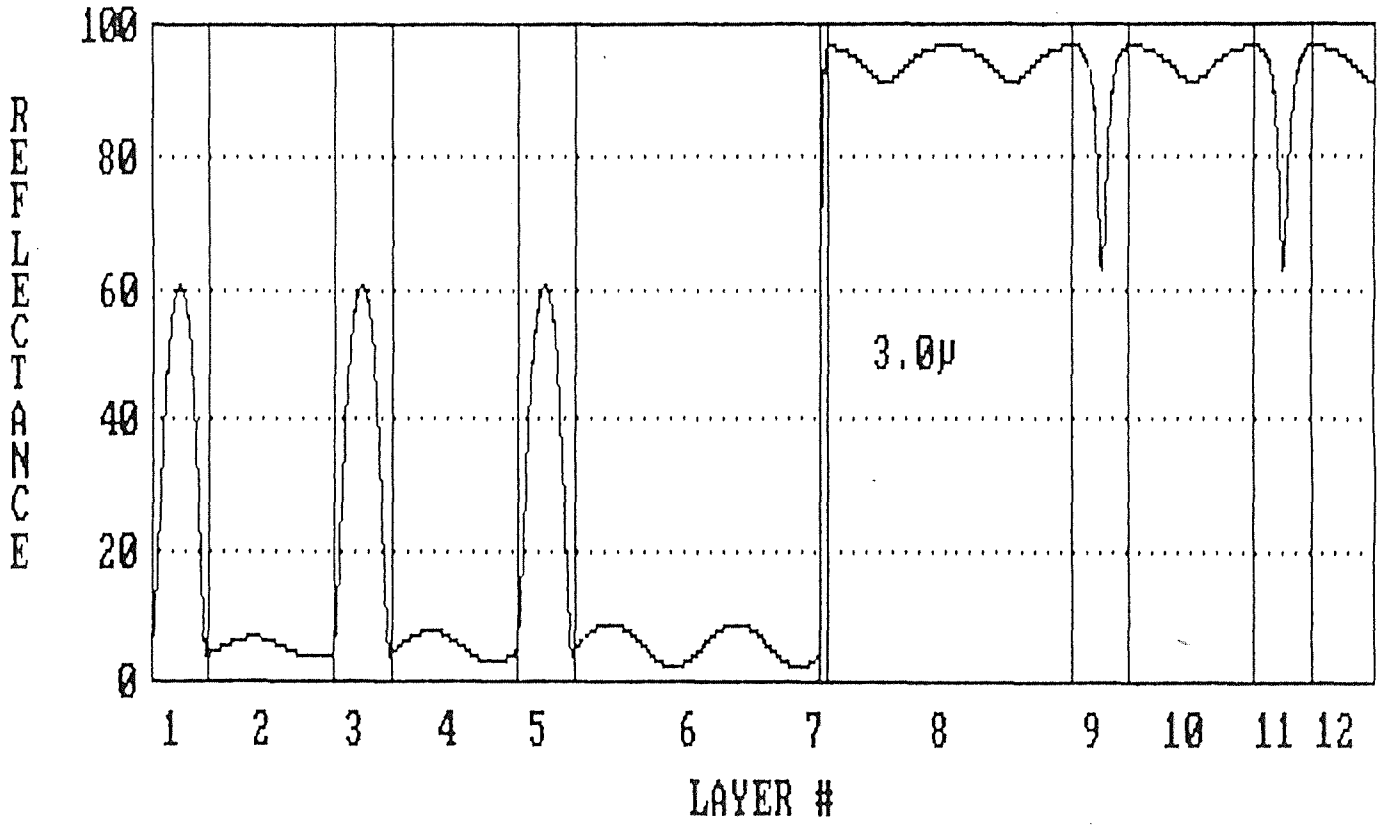

Figure 1 Optical monitoring curve for the filter with peak transmission at 3.0 μm. Monitoring wavelength is 1.5 μm. Layer 1 is silicon.

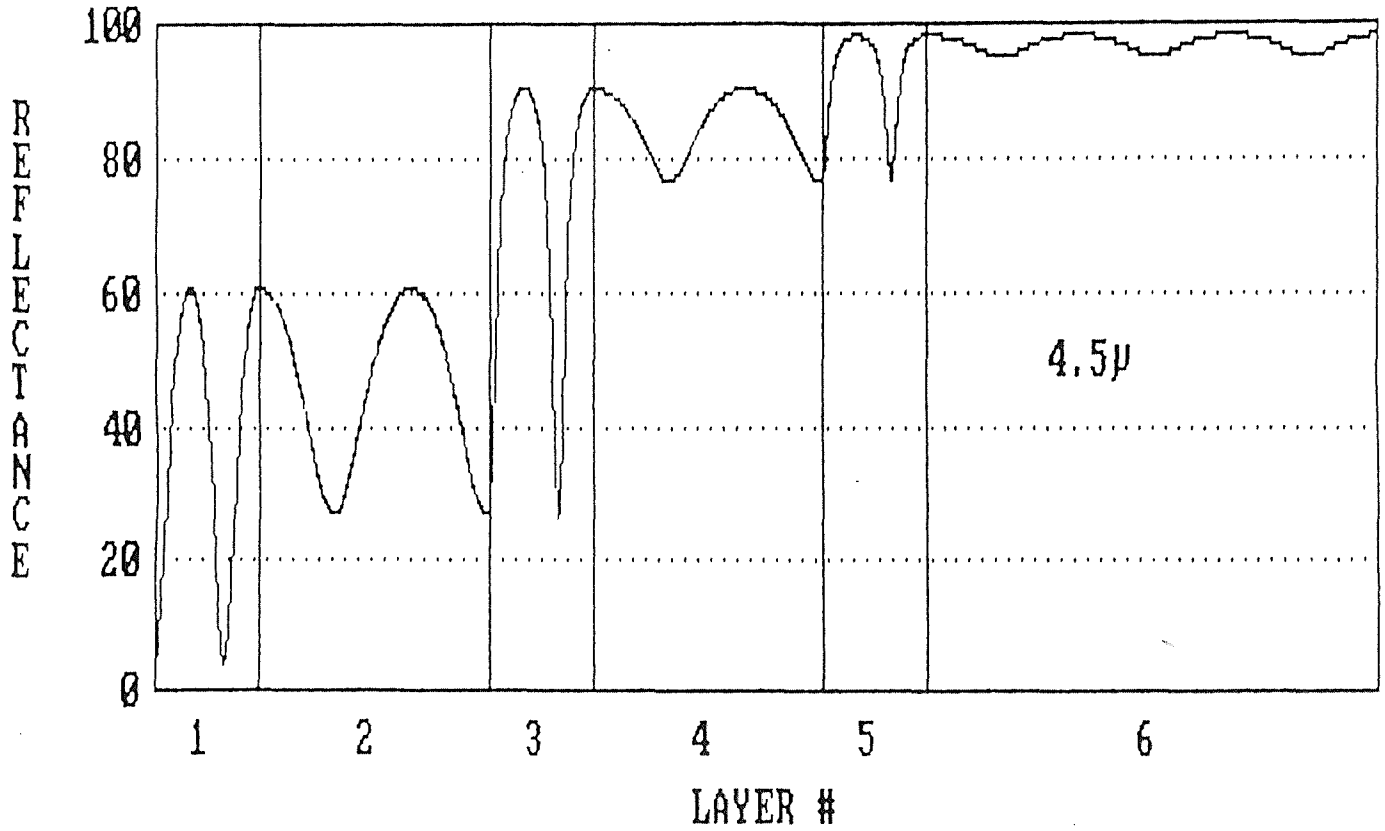

Figure 2 (a) Optical monitoring signal for filter with peak transmission at 4.5 μm. Layer 1 is silicon. Monitoring signal is 1.5 μm. This is for the first test piece.

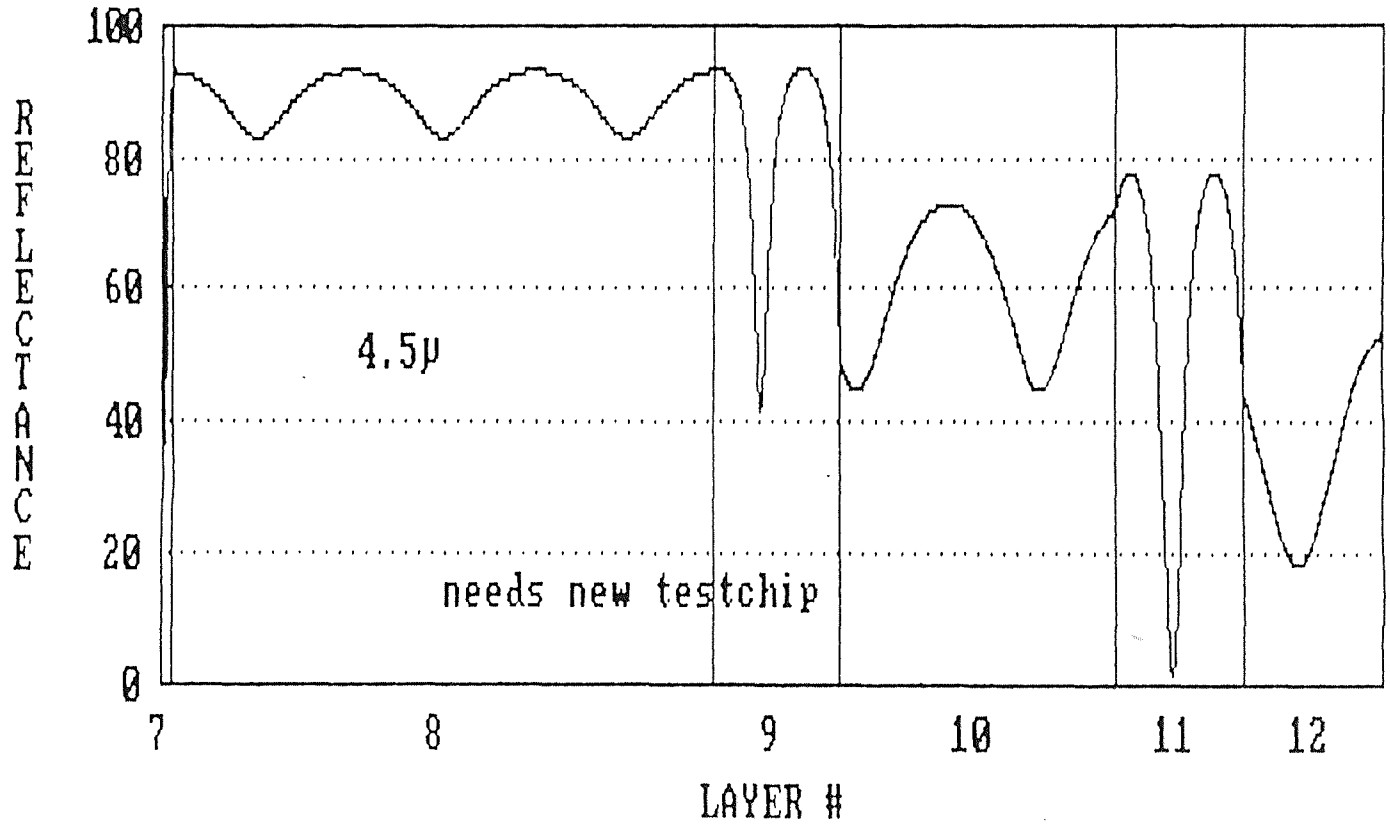

Figure 2 (b) Optical monitoring curve for the filter with peak transmission at 4.5 μm. This curve is simulated for the second test piece.

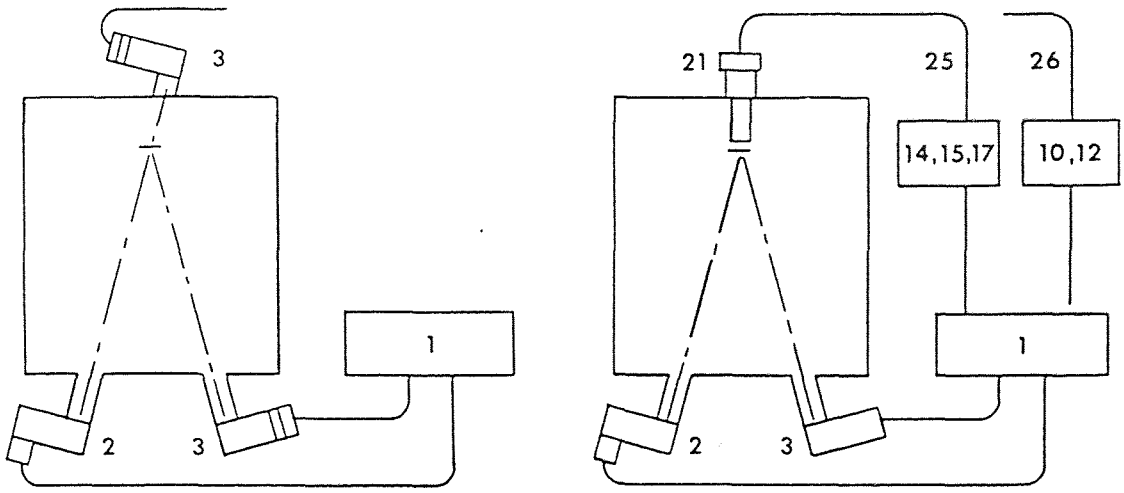

(a) (b)

Figure 3 (a) Basic system. (b) System with fiber optics.

System with Fiber Optics

The monitor may also be used with fiber optics accessories (Figure 3b). A fiber optic "vacuum well " (21) may be installed to use either a single channel cable (25) for light transmission detection, or a dual channel cable (26) for back reflection monitoring. Item 25 requires a transmission detector unit (14), a basic detector with filter position, (15) with selectable filters in a rotary filter wheel or (17) with monochromator. Both 15 and 17 are available with remote and computer compatible operation. For back reflection with a dual cable (26), a light source and detector unit is required, either with a selectable filter capability (10) or monochromator(12), both available with remote actuation and computer compatibility.

The monitor system may be set up for a combination of reflective monitoring using (2) and (3), and transmission sensing using (14), (15),or(17). Reflection and transmission are not operable simultaneously, but may be switched in a manual multiplex mode for cross checking. Another system variation includes with back reflection fiber optics (26) and (10) or (12).

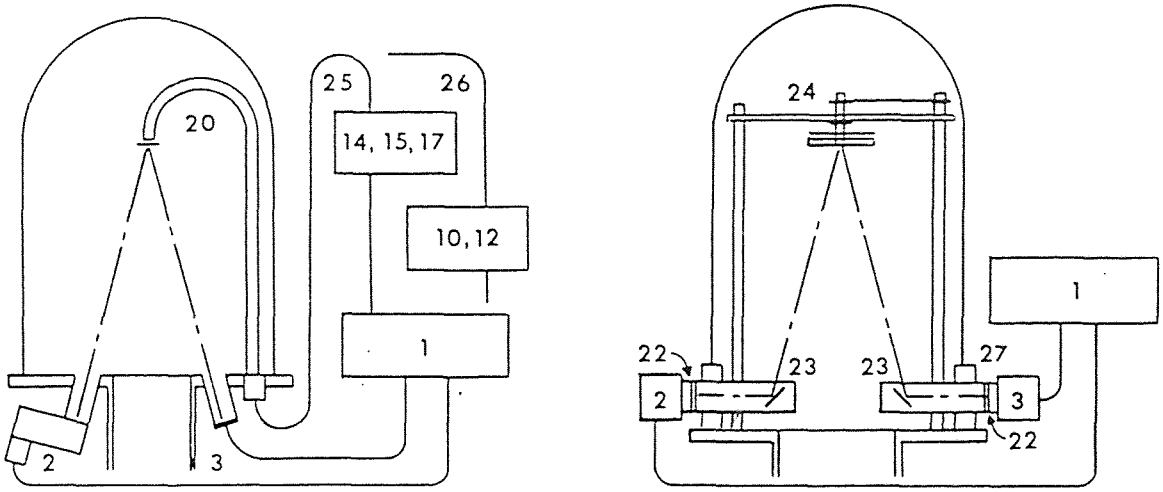

(a) (b)

Figure 4 (a) Bell jar installation. (b) Bell jar accessories.

Bell Jar Installation

The "bell jar" type of installation using a baseplate vacuum seal for the fiber optic well avoids the errors in location that are possible in an installation in the top of a bell jar (Figure 4a). This "J" well configuration is available with the fiber optics window position as required. The standard design window may be located up to 30 inches above the compression seal with up to 12 inches between the axis of the main well tube and the optical port.

Bell Jar Accessories

The bell jar arrangement includes equipment and fittings for a "collar" (27) installation (Figure 4b). Source and receiver units (2) and (3) are mounted on vacuum window retainer rings (22). Adjustable mirror beam deflectors (23) are mounted inside the collar and a manually operated chip changer (24) is mounted in the baseplate. Fiber optics may also be utilized with this installation using the "j" well (20) and the other fiber optics units.

APPENDIX V

FTS 60 -FTIR SPECTROMETER

General Description

FTS 60 is a versatile, bench-top, research-grade FT-IR system with powerful, expandable data system, configured for the mid-infrared region (4400-450 cm^{-1}) and expandable to 10,000-250 cm^{-1}

Each system consists of a compact data system, operator terminal and an optical console. The data system includes a Digilab 3260 data system, designed around the Motorola 68000 microprocessor, running under IDRIS TM, UNIX ™ like operating system, optimized for efficiency and real time applications. 1 Mbyte memory is standard, and may be increased in 0.5 Mbyte increments. Data and program storage is provided by a 40 Mbyte Winchester disk, and a 1 Mbyte floppy disk. The system also contains a 13" color raster display, and a keyboard with a full ASCII character set and, in addition , 14 function keys, 16 other dedicated keys, and a joystick for control of the spectral display. A four color digital and plotter and 120 cps dot matrix printer are standard.

The optical console includes a 60° Michelson interferometer, rapid purge design, and resolution selectable up to 0.5cm^{-1}. A mirror flipper can divert the collimated IR beam into optional auxillary consoles - a research-grade GC accessory, second sample compartment, permanently mounted microscope accessory etc. A high temperature ceramic source and efficient optics deliver 110 mW IR power at the sample.

FT-IR software application packages include a "C" language compiler, and documentations. The values of the optical constants are calculated from the transmission or reflectance data using the following program:

```
C*************************************************************
C     PROGRAM NEWNK
C
C     CALCULATION OF OPTICAL CONSTANTS N & K FOR THIN
      ABSORBING FILMS ON A THICK TRANSPARENT SUBSTRATE
C     BASED ON THE PROCEDURE OUTLINED BY S.G. TOMLIN IN :
C           BRIT. J. APPL. PHYS (J. PHYS. D)  1667 (1968)

C     WRITTEN BY W.R. FRENCHU/REVISED BY P.J. ZANZUCCHI
      (1/20/92).
C     COPYRIGHT (C) 1988 - DAVID SARNOFF RESEARCH CENTER
C     ALL RIGHTS RESERVED.
C*************************************************************
C
      REAL LAMBDA, N1, N2, N1SQ, N2SQ, N1N2, NINC, NSTART,
      K1, K1SQ, NEND &, NHOLD
      INTEGER F1F, HEAD (30), RFLAG, ODF
C
C*************************************************************
C     PROGRAM CONSTRAINTS AND INITIALIZATION
C*************************************************************
C
      OPEN(UNIT = 16, FILE= 'NEWNK.OUT')
      OPEN(UNIT = 17, FILE = 'NEWNK.DAT')
      LAMBDA = 0.0
C
C*************************************************************
C     DATA FILE STRUCTURE (NO FORMAT)
C     ------------------------------------------------
C     HEADER
C     N2, NSTART, NEND    (SUBSTRATE INDEX, RANGE FOR N
      SEARCH)
C     D                   (THICKNESS)
C     ODF                 (1 IF OD DATA, ELSE 0)

C     NINC, EPSLON,       (N1 INCREMENT, EPSILON FOR F2 FIT)
C     LAMBDA, REFLECTANCE OF AL(% ABS), R DATA, T DATA
C*************************************************************
```

```
C
      READ(17,996)  (HEAD(I), I= 1,30)
      WRITE(6,995)  (HEAD(I), I= 1, 30)
      WRITE(16,995)  (HEAD(I), I=1,30)
      WRITE(16,997)
      READ(17, *) N2, NSTART, NEND
      N2SQ = N2*N2
      RB= ((N2-1.)/(N2+1.))**2
      READ(17,*) D]
      READ(17,*) ODF
      READ(17,*) NINC,EPSILON
      WRITE(16,992) D
      WRITE(16,993) NSTART,NEND
      WRITE(16,991) NINC,EPSILON
      WRITE(16,987) N2
      IF (ODF.EQ.1) WRITE (16,990)
      IF (ODF.NE.1) WRITE (16,989)
      WRITE(16,997)
      WRITE(16,998)
C
C*****************************************************************
C     NEW LAMBDA
C*****************************************************************
C
10    READ(17, *, END= 9999, ERR= 9998) LAMBDA, RREF,RO,TO
      WRITE (16,997)
      IF(ODF.NE.1) GOTO 20
      RO = 10.**(-1.*R0)
      TO = 10.**(-1.*T0)
20    R0 = R0*RREF
      RFLAG = 0
      F1 = 0
      CON = 4.*3.141592*D/LAMBDA
      F1F = 0
      N1= NTART - NINC
      GOTO 501
C*****************************************************************
C     INCREMENT N1
C*****************************************************************
```

```
C
500   F1F = 1
      OLDF1 = F1
501   N1= N1 + NINC
      IF(N1.GT.NEND) GOTO 10
502   N1SQ = N1*N1
      RA= ((N1 - N2)/(N1 + N2))**2
      T= T0*(1.-RA*RB)/(1.-RB)
      R= R0-RB*T*T/(1.-RA*RB)
      IF((R+T).GT.1)R = 1.-T
      A3= 2.*N2*(R-1.)/T
      TWOGAM = CON*N1
      SIN2GM =SIN(TWOGAM)
      COS2GM= COS(TWOGAM)
      N1N2= N1*N2
      B1= N1SQ*N2
      B2= 2.*N1N2
C
C*****************************************************************
C     STARTING VALUE FOR K1
C*****************************************************************
      K1 = 0
1000  K1SQ= K1*K1
      SUM = N1SQ + K1SQ
      DIF= SUM-N2SQ
      EXP2AL = EXP(CON*K1)
      A= (SUM + N2SQ)*TWOGAM/2
      B= K1*N1 + N1N2*TWOGAM
C
C*****************************************************************
C     CALCULATE DERIVATIVE
C*****************************************************************
      F2P = 2.*A3*K1 + (A+B)*EXP2AL+(A-B)/EXP2AL
     & + (DIF + 2.*K1SQ)*SIN2GM + 4.*N2*K1*COS2GM
C
C*****************************************************************
C     CALCULATE F2(N2,N1)
C*****************************************************************
C
```

```
      A1 = (SUM +N2SQ)*TWOGAM/2.
      F2 = SUM*A3 + (A1 + B1)*EXP2AL +  (B1 - A1)/EXP2AL
     & +K1*DIF*SIN2GM + 2.*N28K1SQ*COS2GM
C
C*****************************************************************
      SOLUTION ?
C*****************************************************************
C
      IF(ABS(F2/F2P).LT.EPSLON) GOTO 2000
C
C*****************************************************************
C     NO: ADJUST K1 AND RESTART
C*****************************************************************
C
      K1 = K1 - F2/F2P
      GOTO 1000
C*****************************************************************
C     YES: CALCULATE F1(N1, K1)
C*****************************************************************
C
2000  A2 = N2SQ + SUM
      F1 = (-4.)*N2*SUM*(1.+ R)/T +(1.+ SUM)/2.*((A2 + B2)*EXP2AL
     & +(A2 - B2)/EXP2AL) + (1.- SUM)*(DIF*COS2GM -  2.*N2*K1
     & *SIN2GM)
      IF(RFLAG.EQ.1) GOTO 3500
      IF(FIF.EQ.0) GOTO 500
C
C*****************************************************************
C     ON SIGN CHANGE BOTH EQUATIONS HAVE ZEROED
C*****************************************************************
C
      IF(OLDF1*F1.LT.0) GOTO 3000
C
C*****************************************************************
C     NO ROOT
C*****************************************************************
      OLDF1 = F1
      GOTO 500
C*****************************************************************
```

```
C     ROOT FOUND
C*************************************************************
C
3000  RFLAG = 1
      FHOLD = F1
      NHOLD = N1
      N1 = N1 - N1NC*F1/(ABS(F1 - OLDF1))
      GOTO 502
3500  ALPHA = CON/D*10000*K1
      WRITE(16,999)LAMBDA,N1,K1,ALPHA,F1,F2
      RFLAG = 0
      F1 = FHOLD
      N1 = NHOLD
      GO TO 500
C
987   FORMAT(1X,' SUBSTRATE INDEX = ',F4.2)
988   FORMAT(1X,'NEWNK: **READ ERROR AT LAMBDA=',F7.4,'**')
989   FORMAT(1X,'(ORIGINAL DATA IN PERCENT
      TRANSMITTANCE)')
990   FORMAT(1X,'(ORIGINAL DATA IN OPTICAL DENSITY)')
991   FORMAT(1X,'N INCREMENT =', F6.4,
      & /1X,'F2 EPSILON =', 1PE8.2)
992   FORMAT(1X,'THICKNESS =', F6.4, 'MICRONS')
993   FORMAT(1X,'SOLUTIONS FOR N =', F4.2, 'TO', F4.2)
995   FORMAT(/11H NEWNK V1.0,/1X,30A2)
996   FORMAT(30A2)
997   FORMAT(1X)
998   FORMAT(/,'LAMBDA',4X, 'N',7X, 'K',8X, 'ALPHA',7X, 'F1',9X,'F2')
999   FORMAT(1X,F5.3,2X,F5.2,4(2X,1PE9.2))
C
9998  WRITE(6,998) LAMBDA
9999  STOP
      END
```

BIBLIOGRAPHY

1. Jamieson, J.A., R.H. McFee, G.N. Plass, R.H. Grube, and R.G. Richards. *Infrared Physics and Engineering.* New York: McGraw-Hill (1963).

2. Hudson, R.D. *Infrared System Engineering.* New York: Wiley (1969).

3. Macleod, H.A. *Thin-Film Optical Filters.* New York: McGraw-Hill (1989).

4. Singh, B., P.R. Denton, R.T Vaughan, and R.H. Williams. "Use of Fiber Optics in Optical Monitoring." Proc. of Soc.Vac. Coaters. 26 (1983).

5. Jacquinot P. "The Luminosity of Spectrometers with Prisms, Gratings or Fabry-Perot etalons" J. Opt. Soc. Am. 44 (1954): 761-5.

6. Houghton, J.T. and S.D. Smith. *Infrared Physics.* London: Oxford (1966).

7. Hadni, A. *Essentials of Modern Physics Applied to the Study of the Infrared.* Oxford: Pergamon (1967).

8. McCleese, D.J., J.T Schofield, R.W Zurek, J.V. Martonchik, R.D. Haskins, D.A. Paige, R.A. West, D.J. Diner, J.R. Locke, M.P. Chrisp, W. Willis, C.B. Leovy, and F. W. Taylor "Remote sensing of the atmosphere of Mars using infrared pressure modulation and filter radiometry." Appl. Opt. 25 (1986): 4232-45.

9. Pulker, H.K. *Coatings on Glass.* Amsterdam: Elsevier (1984).

10. Haus, H.A. *Waves and Fields In Optoelectronics.* New Jersey: Prentice-Hall(1984).

11. Berning, P.H. and A.F. Turner "Induced transmission in absorbing films applied to band pass filter design." J. Opt. Soc. Am. 47(1957): 230-9.

12. Macleod, H.A. "Monitoring of optical coatings." Appl. Opt. 20(1981): 82-9.

13. Heavens, O.S. *Optical Properties of Thin Solid Films.* New York: Dover (1965).

14. Holland, L. *Vacuum Deposition of Thin Films.* New York: Wiley (1965).

15. Murthy, T.G.K., H.N. Rao, and K.S.R. Anjaneyulu "A new approach for the thickness monitoring of optical thin films." Vacuum 22(1972): 151.

16. Macleod, H.A. and E. Pelletier "Error compensation mechanisms in some thin-film monitoring systems." Optica Acta 24(1977): 907-30.

17. Skettrup, T. "Optical monitoring of nonquarterwave stacks." Opt. Engg. 26(1987): 1175-81.

18. Behrndt, K.H. *Physics of Thin Films.* (Eds. G. Hass and R.E. Thun) New York: Academic (1966).

19. Ritchie, F.S., Ph.D Thesis, U. Reading (1970).

20. Sauerbrey, G. Physikal Verhandl., 8(1957): 113.

21. Lostis, P. Rev. Optique(1959): 38.

22. Stockbridge, C.D. *Vacuum Microbalance Techniques.* (Ed. K.H. Behrndt) New York: Plenum (1966).

23. Ramadan, B., Piyakis, K., and J.F. Kos "High accuracy quartz crystal thin film monitor." Rev. Sci. Instrum. 50(1979): 867-71.

24. Heyman, J.S. and W.E. Miller "Effects of accumulated film layers on the accuracy of quartz film thickness monitors." J. Vac. Sci. Technol. 15(1978): 219-22.

25. Frankena, H.J. and C.J. vd Laan "Monitoring of optical thin films using a quartz crystal monitor." Vacuum 27(1977): 391-7.

26. Collyer, P.W. "Selection and Processing of Infrared Materials" Appl. Opt. 5(1966): 765-70.

27. Bates, J.B. "Fourier Transform Infrared Spectroscopy." Science 191(1976): 31-7.

28. Bates, J.B. *Fourier Transform Infrared Spectroscopy: Applications to Chemical Systems.* New York: Academic (1978).

29. Finkelnburg, W. J. Opt. Soc. Am. 39(1949): 185-6.

30. McMahon, H.O. "Thermal radiation from partially transparent reflecting bodies." J. Opt. Soc. Am. 40(1950): 376-80.

31. Gardon, R. J. Am. Ceram. Soc. 39(1956): 278-87.

32. Rodgers, J.L. High Temp. - High Pressures 4(1972): 271-80.

33. Barr, J.K. Infrared Phys. 9(1969): 97-108.

34. Hordvik, A and L. Skolnik, Appl. Opt. 16(1977): 2919.

35. Palik, E.D. *Handbook of Optical Constants of Solids.* New York: Academic (1985).

36. Becker, M. and H.Y. Fan *Infrared Optical Properties of Silicon and Germanium.* (Ed. H.K. Henisch) London: Butterworth (1951).

37. Pliskin, W.A. "Fused glass penetration into thermally grown silicon dioxide films." J. Electrochem Soc., 114(1967): 620-23.

38. Pliskin, W.A. "The stability of glazed silicon surfaces to water attack" Proc. IEEE, 52(1964): 1468-71.

39. Loewenstein, E.V. "Optical properties of Sapphire in the far infrared." J. Opt. Soc. Am., 51(1961): 108-12.

40 Wolfe, W.L. and G.J. Zissis (Eds.) *The Infrared Handbook.* Michigan: ERIM (1989).